EXPERIMENTAL EVALUATION OF DYNAMIC INTERLAMINAR G_{IC} OF GLASS FABRIC REINFORCED EPOXY LAMINATES

by

J. S. R. K. T. PRASAD

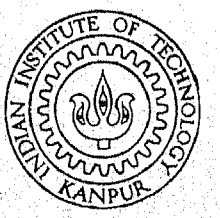

DEPARTMENT OF MECHANICAL ENGINEERING

INDIAN INSTITUTE OF TECHNOLOGY KANPUR

APRIL 1990

EXPERIMENTAL EVALUATION OF DYNAMIC INTERLAMINAR G_{Ic} OF GLASS FABRIC REINFORCED EPOXY LAMINATES

A Thesis Submitted
in partial Fulfilment of the Requirements
for the Degree of

MASTER OF TECHNOLOGY

by

J.S.R.K.T. Prasad

to the

DEPARTMENT OF MECHANICAL ENGINEERING
INDIAN INSITITUTE OF TECHNOLOGY, KANPUR

APRIL, 1990

ME-1990-M-PRA-EXP

CERTIFICATE

This is to certify that the thesis entitled **"EXPERIMENTAL EVALUATION OF DYNAMIC INTERLAMINAR G_{Ic} OF GLASS FABRIC REINFORCED EPOXY LAMINATES"**, by J.S.R.K.T. Prasad, is a bonafied record of work done by him under my guidance and supervision for the award of the degree of Master of Technology in the Indian Institute of Technology, Kanpur. The work carried out in this thesis has not been submitted elsewhere for the award of a degree.

Prashant Kumar

Dr. Prashant Kumar
Professor
Dept. of Mech. Engg.
I.I.T. Kanpur

(THESIS SUPERVISOR)

ABSTRACT

An experimental set-up had been designed, constructed and perfected to measure dynamic G_{Ic}. Double cantilever beam specimen of glass fabric reinforced laminate with a sharpened artificial crack was loaded dynamically by dropping a weight on the stopper attached to the lower cantilever of the specimen through an incident load bar. The upper cantilever was attached to a transmitted load bar, suspended from the roof. The loads and velocities of the cantilever tips were determined by recording stress pulses through strain gauges bonded to the load bars. The crack velocities were in the range of 20 to 100 m/s. At these crack velocities value of G_{Ic} was found to be very small. But specimen required large amount of work input to reach high run away crack velocities.

ACKNOWLDGMENTS

I express my deep sense of gratitude and appreciation to Professor Prashant Kumar, for his valuable guidance throughout the present work. His generous attitude has been a constant source of inspiration and encouragement.

I am thankful to Dr. Badri Rai, Mr. Srivastava, Mr. Sharad C Gupta, Mr. D.K. Sarkar, for the help rendered in the experimental investigation.

It is pleasure to recall my association with my friends Anil K. Gawahale, Suresh Babu, Sanjay Verma and their wonderful help throughout my period of study.

Thanks to Mr. P.N. Pandey, Mr. B.D. Pandey, for the help rendered in making the fine experimental set-up.

I am thankful to other staff members of E.S.A. Laboratory for their help during my work.

I am also thankful to Mr. Sudhir K. Srivastava for nice typing of the manuscript.

- J.S.R.K.T. Prasad

CONTENTS

LIST OF FIGURES

LIST OF TABLES

NOMENCLATURE

G	energy release rate
G_{Ic}	energy release rate in mode I
ϕ	potential energy
U	elastic strain energy stored in the specimen
W_{ext}	work supplied by external force
δ_ϕ	change in potential energy
δ_A	increment in crack area
δ_a	increment in crack length
m_o	mass of the dropping weight
m	cantilever mass of weight and load bar
P	force applied by cantilever weight
v	velocity of platform
v_o	velocity of dropping weight
b	width of the specimen
a	crack length
E_i	energy at the point i
u_i	crack opening displacement at point i
K_i	kinetic energies of the specimen at point i
E	Young's modulus
I	monent of inertia
A_i	cross sectional areas of load bar
σ_i	stress at point i
	mass density of mild steel
c	velocity of stress waves in mild steel
v_i	velocity of the point i
C	compliance of the cantilever
δ	displacement
d_t	increment in time
t	time

CHAPTER 1

INTRODUCTION

1.1 Fibre Reinforced Laminate

A composite material is created by assembly of two or more components - a selected reinforcing agent and a compatible matrix binder. This can achieve a combination of properties not achievable by any of the component materials acting alone.

Since these laminated fibre composites offer atractive properties such as high specific strength and stiffness, now they are increasingly used in structural members of the Aircrafts, Rockets etc.

The growing demand lead to the development of more sophisticated constituent materials and better designs. Major problem in using laminates is that they are susceptible to impact damage which occurs delamination in other words separation of laminae. So delamination resistance has been the important issue for reliability and durability of the composite materials used in structures.

1.2 Mechanisms of Failure

The failure mode depends on the type of loading and micro-structure of the composite such as fibre diameter fibre distribution etc. Volume fraction of fibres also plays an important role. Generally, the following mechanisms of failures will be detected under microscopic observation. (i) breaking of the fibre, (ii) microcracking of the matrix, (iii) separation of fibres from the matrix (debonding) and (iv) delamination. The modes may act separately or jointly [1].

1.3 Failure by Delamination

Delamination takes place through the surface where fibres are effectively absent. The separation of plies can occur under mechanical, thermal or environmental loading. Geometric discontinuities, processing and machining defects etc. also initiate interlaminar cracks. Another major cause for delamination is impact loading on a laminate. At the interlaminar region, the presence of defects such as microcracks, voids and inclusions cause discontinuities in material properties and stresses. The interlaminar strength is, thus, reduced. Interlaminar failure may occur by means of the three well know modes (Fig. 1.1). In mode I failure is produced by a tensile 8 stress applied at right angle to the laminate plane, resulting in opening up of the laminate. In Mode II failure is caused by an in-plane shear stress (forwarded shear mode). In the mode III failure is in antiplane shear stress (parallel to shear mode). Generally, a failure is caused by the combination of all the three modes but delamination failure is known to be caused mainly by modes I and II.

1.4 Fracture analysis of Delamination

In fracture mechanics, mainly two terms were defined to judge the characteristics of an existing crack in the material. One is stress intensity factor (K) which is defined for elastic stress around the crack tip. But stress analysis in composite material is difficult because of local heterogeneity and anisotropy. Thus, it has become necessary to characterize interlaminar fracture with energy release rate (G) which is measurable by experiments. For this constitutive properties of the system are not needed.

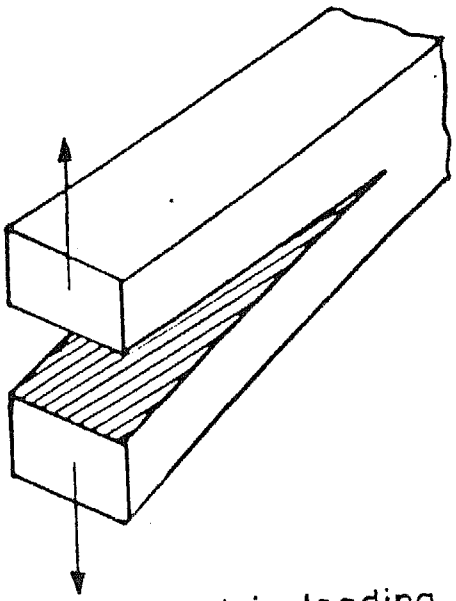

(a) Mode I: symmetric loading
(opening mode)

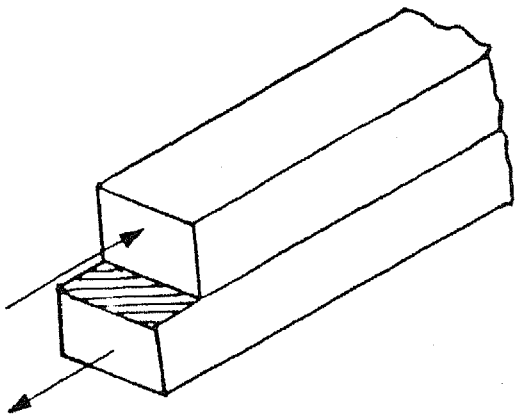

(b) Mode II : skew symmetric
shear loading
(forward shear mode)

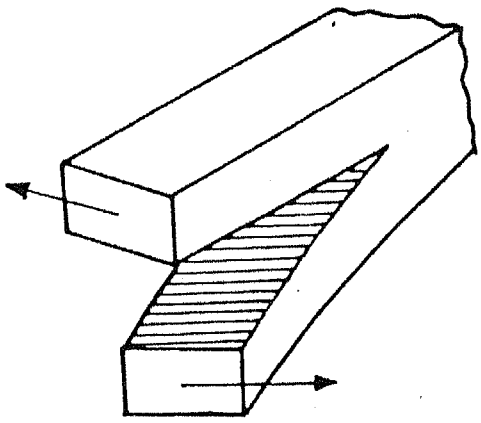

(c) Mode III : antiplane shear loading
(parallel shear mode)

Fig. 1.1 Modes of Crack Surface Displacement

1.5 Determination of Energy Release Rate

Many methods have been established to find out the interlaminar fracture toughness. But these methods are well established under quasistatic conditions. For mode III fracture, methods are not developed because its need has not been felt. For evaluating G_{Ic}, in composite materials, double cantilever beam (DCB) configuration is most commonly used.

Keary et.al. [2] used (DCB) specimen to measure interlaminar fracture toughness in mode I. In order to characterize the behaviour of the delamination and fracture analysis for different modes, Wilkins et.al. [3] found critical strain energy release rate in delamination modes I and II. A DCB specimen was used in mode I testing. Han and Koutsky [4] obtain the interlaminar fracture energy values in case of glass fibre reinforced polyester composite. Devile, Schapery and Bradley [5] developed in nonlinear theory for energy release rate using DCB specimen.

A comparative study of different test methods for fracture toughness in mode I using DCB specimens was carried out by Guedea et. al. [6]. Charenteray and Benzeggagh [7] improved the accuracy in monitoring the crack propagation in mode I using acoustic emission techniques. Narayan [8] used DCB specimen made of glass fibre reinforced composites (GFRC) to evaluate G_{Ic}. Recently R.A. Savanur [9] developed an experimental technique for finding out dynamic G_{Ic} using DCB specimens.

Due to the dependence of G_{Ic} on crack velocity, the variation of velocity of the crack propagating dynamically has been given a deeper thought.

1.6 Out Line of the Present Work

In the present work DCB specimens made from glass fabric

reinforced epoxy laminates ($[0°/45°]_{8S}$) with sharpened starter cracks between 7^{th} and 8^{th} plies were loaded dynamically in mode I. An experimental set-up was designed to load the specimen by dropping a weight through an incident load bar. Specimen was suspended from a transmitted load bar. Loads and velocities at the tips of both the cantilevers of the specimen were found by recording stress pulses through strain gauges bonded to the load bars. Fast moving crack front was monitored by conducting gauges bonded at the known intervals on the side of specimen near the crack tip.

In chapter 2 the details of the specimen preparation are presented. In chapter 3 previous work done on this problem and improvements made on that as a part of the present work are discussed. In chapter 3 description of the experimental technique and the details of the experimental set-up are given. The results of the work and discussion are given in chapter 5. Finally conclusions on the present work are given.

CHAPTER 2

G_{Ic} AT LOW CRACK VELOCITIES

2.1 Introduction

Previously experiments were conducted to determine G_{Ic} at low crack velocities. In this connection, the work carried out by, R.A. Savanur is discussed in this chapter. He developed an experimental technique to measure dynamic interlaminar G_{Ic} by loading DCB specimens dynamically with a dropping weight. In Section 2.5 modified analysis and results for his experiments are discussed.

2.2 Specimen material

For the determination of dynamic G_{Ic} he prepared double cantilevered beam (DCB) specimens out of Glass fabric reinforced plastic (GFRP) laminates.

The composite plates were fabricated through the hand lay-up technique. Sixteen layers of fine woven glass fabric with plane weave of 36 x 32 count/inch and 185 g/m^2 area density were wetted with an epoxy (LY 556 with hardener). The resulting laminates ($[0°/90°]_{8S}$) were of 40% fibre volume fraction.

For determining energy release rate in mode I a crack was introduced in the composite laminate by keeping a folded mylar sheet at one end of the midplane during the hand lay-up casting.

2.3 Experimental technique

The technique pulls the two halves of a DCB specimen (Fig. 2.1) apart to propagate the crack. The upper cantilever of the

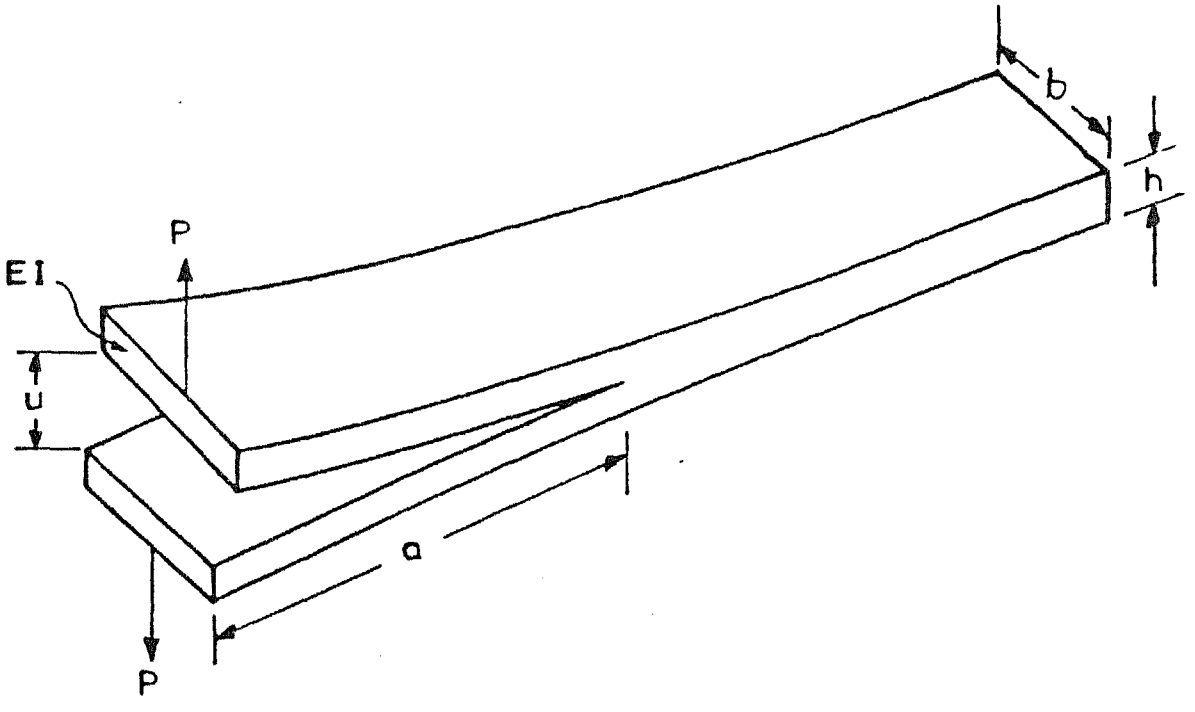

Fig. 2.1 Double Cantilever Beam Specimen

specimen was suspended from a fixed roof while the lower cantilever was loaded by a falling weight guided by load bar. When the weight was dropped from a predetermined height, it impacted the stopper and thus the specimen was loaded dynamically. The schematic diagram of his experimental set-up is shown in Fig. 2.2. The displacement of the lower end of the load bar was measured by LVDT. To monitor the crack propagation he glued four conducting gages by the side of the specimen near the crack tip at regular intervals. These gauges were connected to oscilloscope through an electronic circuit. Fig. 2.3 shows a typical X - Y plot obtained from oscilloscope which gives LVDT record and propagation gauge breakages w.r.t. time. Crack velocity was calculated by the durations of the steps noted from the plot.

2.4 Expression for dynamic G_{Ic}

He used energy balance approach to calculate the dynamic G_{Ic}. The system taken for energy balance contained specimen, load bar and weight. He made the following analysis for the system.

Potential energy ϕ of a specimen with a crack defined as

$$\phi = U - W_{ext} \tag{2.1}$$

where, U is elastic strain energy stored in the specimen and W_{ext} is the work supplied by the external force.

Expression for G_{Ic} is given as,

$$G_{Ic} = - (\delta\phi/\delta A) \tag{2.2}$$

where δA is the increment in crack area because of propagation.

If u is the crack opening displacement (COD), and v_o is the velocity of the dropping weight before it touches stopper, then

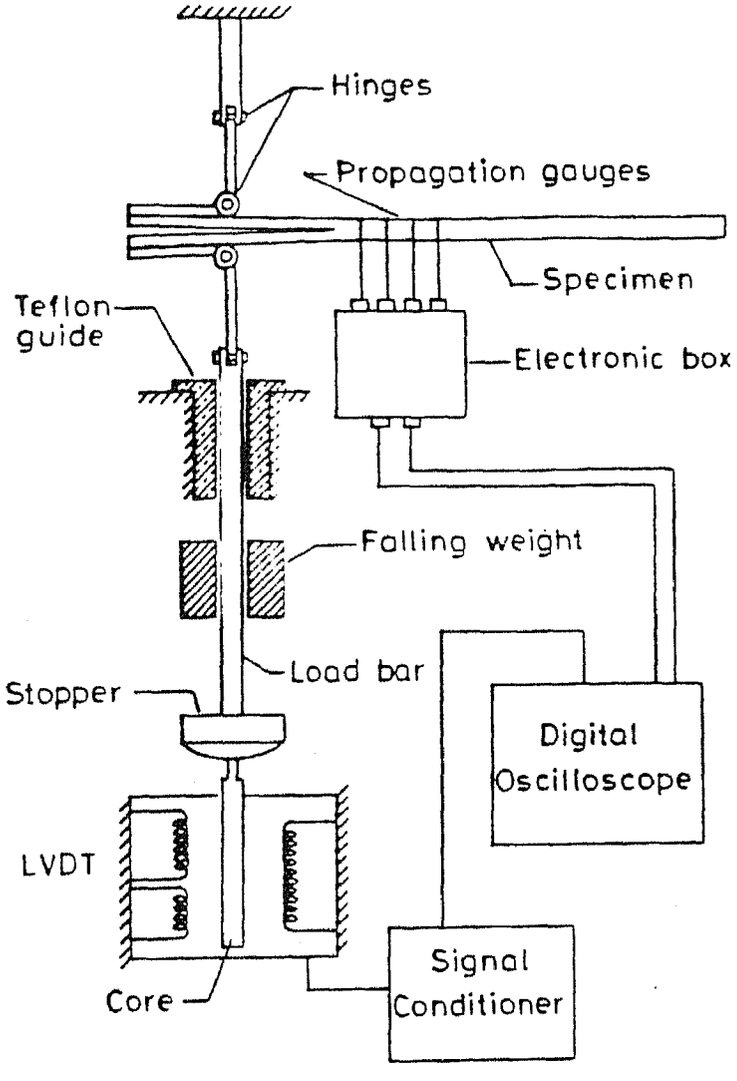

Fig. 2.2 Schematic Diagram of the Experimental Set-up Used by Savanur.

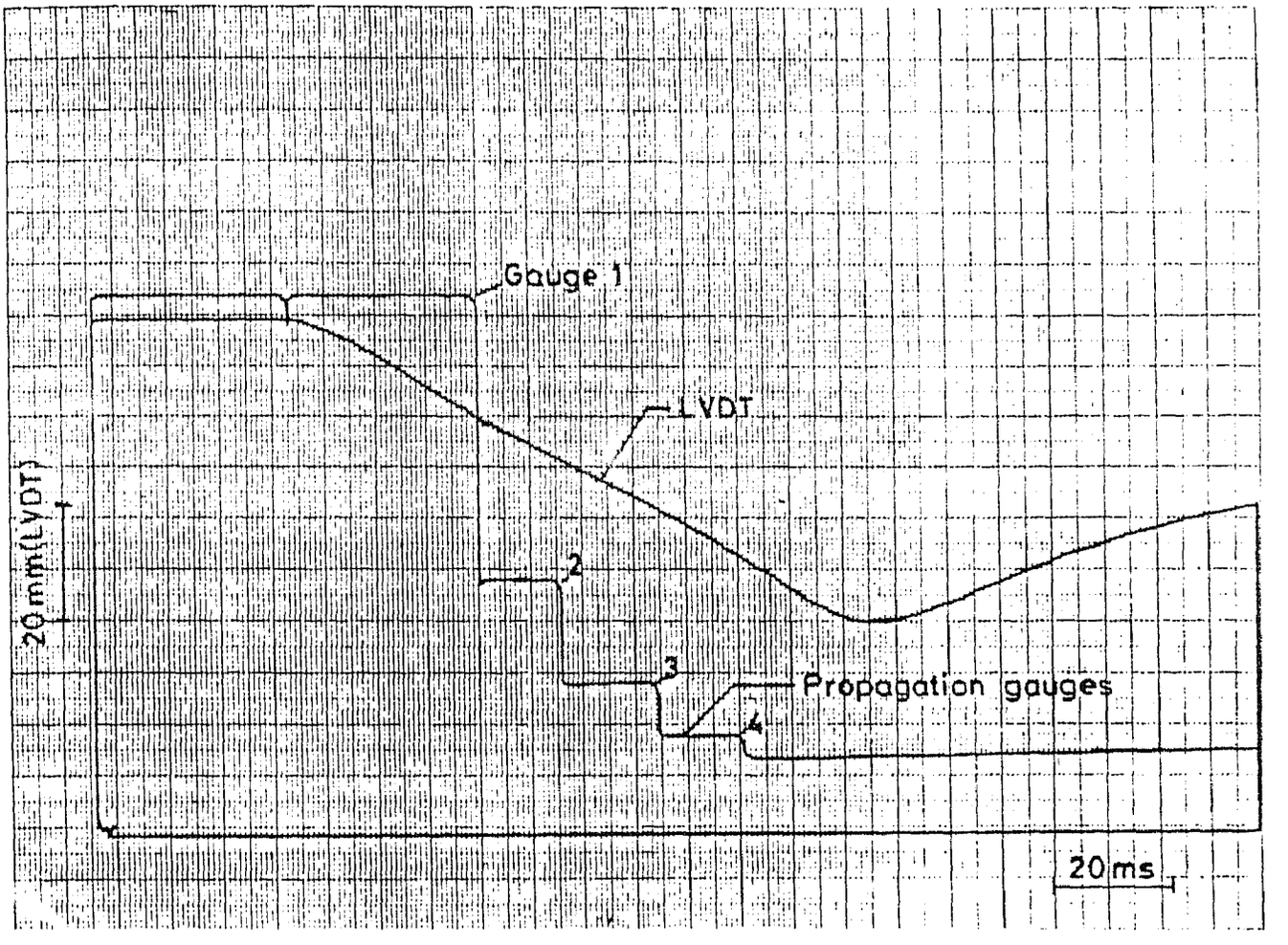

Fig. 2.3 Oscilloscope Traces of LVDT and Propagation Gauges

expression for ϕ changes to

$$\phi = U - [Pu + \tfrac{1}{2} m_o v_o^2 - \tfrac{1}{2} mv^2] \qquad (2.3)$$

where, m_o is mass of the dropping weight, m is combined mass of the weight and load bar, P is the force applied by the combined weight (assumed as mg, where g is acceleration due to gravity) and v is the velocity of the platform. The COD is assumed to be the displacement of the stopper measured by LVDT.

Substituting ½Pu for the strain energy term in Eq. 2.3, one obtains,

$$\phi = - \tfrac{1}{2} Pu - \tfrac{1}{2} m_o v_o^2 + \tfrac{1}{2} mv^2 \qquad (2.4)$$

Differentiating above Eq. w.r.t. 'a' gives,

$$G_{Ic} = (P/2b) \; u/ a \; - \; (m/2b) \; (v^2/ a) \qquad (2.5)$$

where b is the width of the specimen.

In Table 2.1 his experimental data is presented. Fig 2.4 shows the dynamic G_{Ic} variation with crack velocity.

2.5 Modified analysis

Later in the present work it was realized that, few errors were present in the above analysis. Mainly, considering a big system for energy balance involved dynamic losses in load bar, weight etc. And constant load condition is assumed in figuring out the strain energy term. More over kinetic energy change of the specimen was not considered.

So the problem was analized again first by taking kinetic

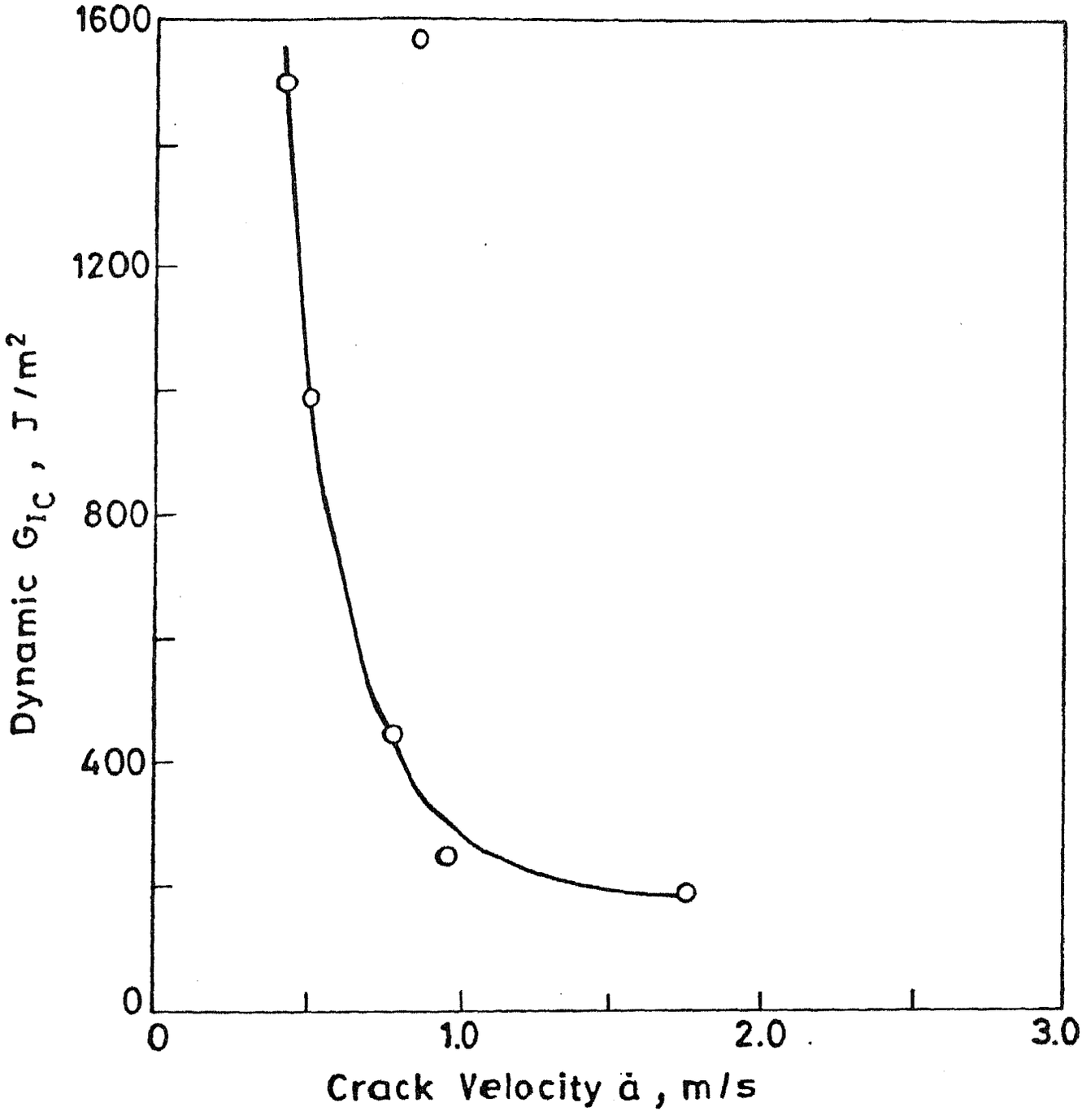

Fig. 2.4 Relation between G_{Ic} and Crack Velocity at the First Propagation Gauge

Table 2.1 Details of Experiments

Expt. No.	Initial Crack length (mm)	Load (kg)		Dropping Height (mm)
		Dropping	Load bar	
S1Ø	5Ø.Ø	2.7Ø3	Ø.298	45
S11	5Ø.5	2.7Ø3	Ø.298	4Ø
S12	51.Ø	3.7Ø5	Ø.298	2Ø
S13	51.Ø	3.7Ø5	Ø.298	25
S15	56.Ø	3.7Ø5	Ø.298	32

Specimen width 3Ø ± Ø.5 mm

Specimen thickness 3 ± Ø.1 mm

distance between the propagation gauges 1Ø ± Ø.5 mm

Where, P is load developed on the cantilever ends and is given by

$$P = \frac{3\ u\ E\ I}{2\ a^3}$$

Substuting it is Eq. (2.1Ø) and differentiating the resulting expresion with respect to a, we obtain

$$\frac{U}{a} = \frac{3\ E\ I}{4}\left[\frac{2\ u}{a^3}\ \frac{du}{da} - \frac{3\ u^2}{a^4}\right]$$

Since the relation between u and a is recorded only for four crack length, a cubic curve is fitted withy the least square method. Based on same deformed configuration of the cantilevers a software program has been developed to determine K/ a by evaluating the particle velocities of specimen.

It was observed that the contribution of the above term in G_{Ic} was considerably low (5% to 8% of the G_{Ic}). Analysing the same data with above approach gave G_{Ic} at low crack velocities near to the static value after imposing some error analysis. Results are presented in Fig. 2.5. Also Expt. S15, showed a much higher error and therefore the results of this experiments may not be taken seriously.

In the present work another approach was followed to isolate the specimen, which is described in the following chapters.

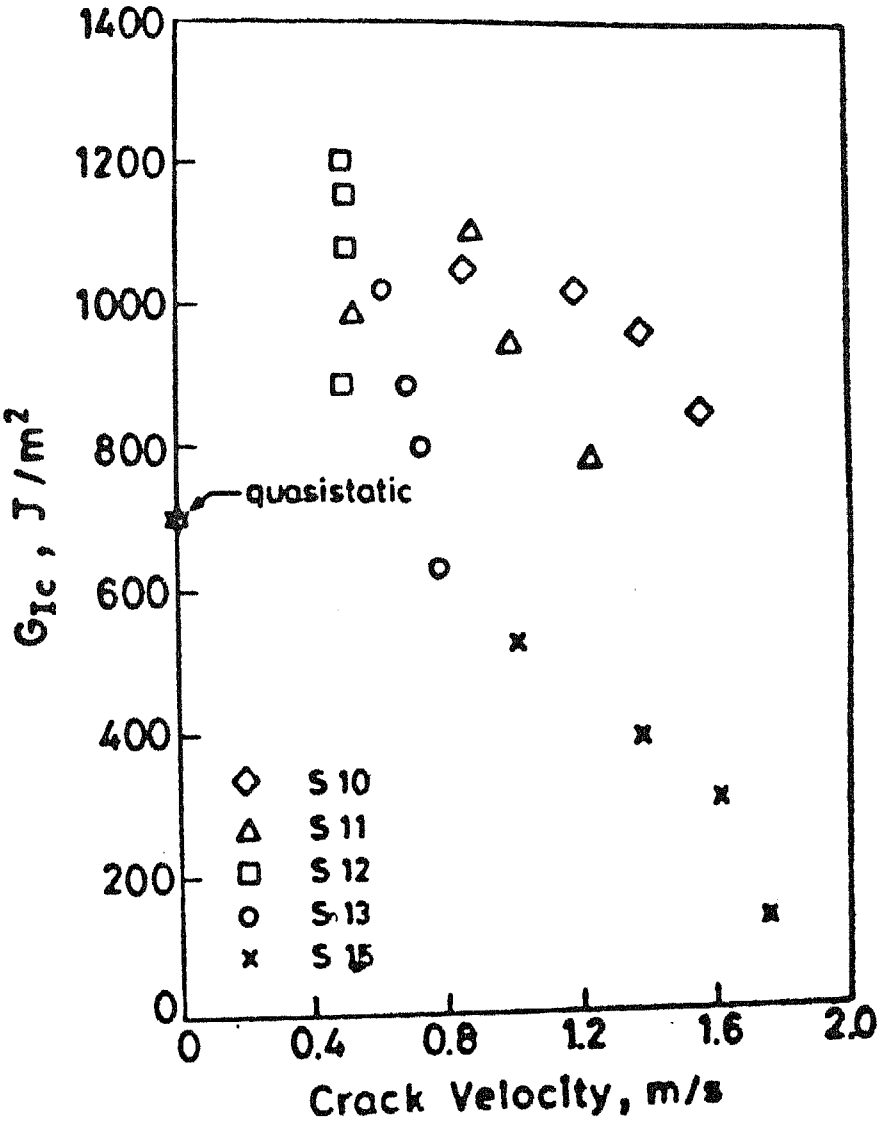

Fig. 2.5 Modified Results

CHAPTER 3

SPECIMEN PREPARATION

Glass fabric reinforced laminates were fabricated in our laboratory , from the prepregs. Prepregs, which are semicured laminae (plies) made from glass fabric reinforcement in epoxy resin were bought from TECH INVEST Pvt.Ltd, Haridwar, U.P. The prepregs were cut to size and stacked in a desired sequence before they were pressed at high pressure and temperature. From these laminates double cantilevered specimens ,of required size , were cut.

3.1 Specifications of prepregs

Fallowing are the specifications of prepreg sheets as provided by supplier.

Reinforcement : Glass fibre fabric finely woven , approximately balanced (36 x 32 counts/inch) with area density 185 gm/m .

Matrix : Epoxy LY556 (Ciba-Geigy, Bombay)
Hardener HT973 ,,
Hardener H 973 ,,

Mixed in the ratio of 100:35:1 respectively.

Width : 1 meter

3.2 Preparation of laminates

The prepreg sheets were cut into pieces of size 220 x 220 mm and 16 layers were stacked one over the other with the desired orientation($[0°/45°]_{8S}$). The stack was placed in a press shown in Fig. 3.1 .

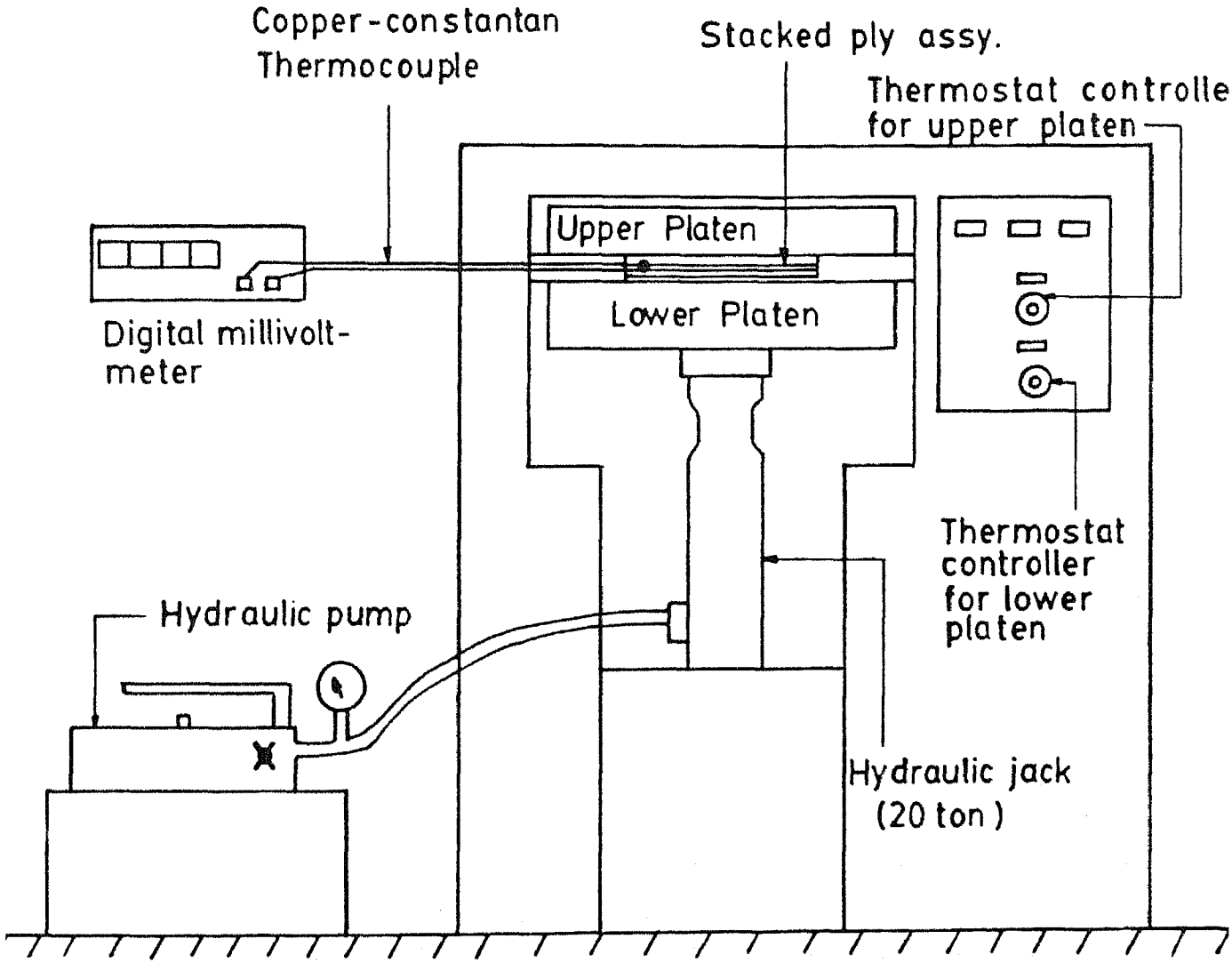

Fig. 3.1 Schematic View of the Press

The press consists of two platens with insulated heaters inside. Regulators for these heaters are placed on a control panel , which is on the top side of the machine frame. Lower platen can be lifted by a jack of 15 ton capacity. It is operated by a manually operated pressure pump. The end of a copper constantan thermocouple was embedded at one side of the prepreg stack to measure temperature. The thermocouple was connected to a digital multimeter to measure temperature in terms of voltage.

Before this stack of prepregs were placed between the platens, it was sandwiched between two nicely polished aluminium plates of about 1.5 mm thick. Also ,a thin release sheet of teflon was inserted on each side of the stack to avoid spreading of epoxy over the surface of the aluminium plates during hot pressing.

A teflon piece of size 240 x 80 mm was also placed between 7^{th} and 8^{th} plies to create artificial crack in the laminate at one edge.

The entire setup was kept on the lower platen of the press and pressure was built up by operating the pump. When the pressure reached 69.04 x 10^{-4} MPa heaters were switched on. Temperature was allowed to reach 150° C which approximately took 45 minutes. Then pressure was increased three times (207.1 x 10^{-4} MPa) and temperature was maintained at 150° C for 2 hours. Then the pressure was released and the laminate was taken out for post curing. It was kept in an oven at 120° C for 3 to 4 hours before it was to cool down to room temperature. The heat and pressure cycles are shown in Figs. 3.2. Later this laminate was cut into specimens of size 30 x 200 mm. The length of the artificial crack is maintained up to 85 mm length (Fig. 3.3a and 3.3b).

3.3 Bonding of Hinges

To pull the specimen in tension ,two hinges made of mild

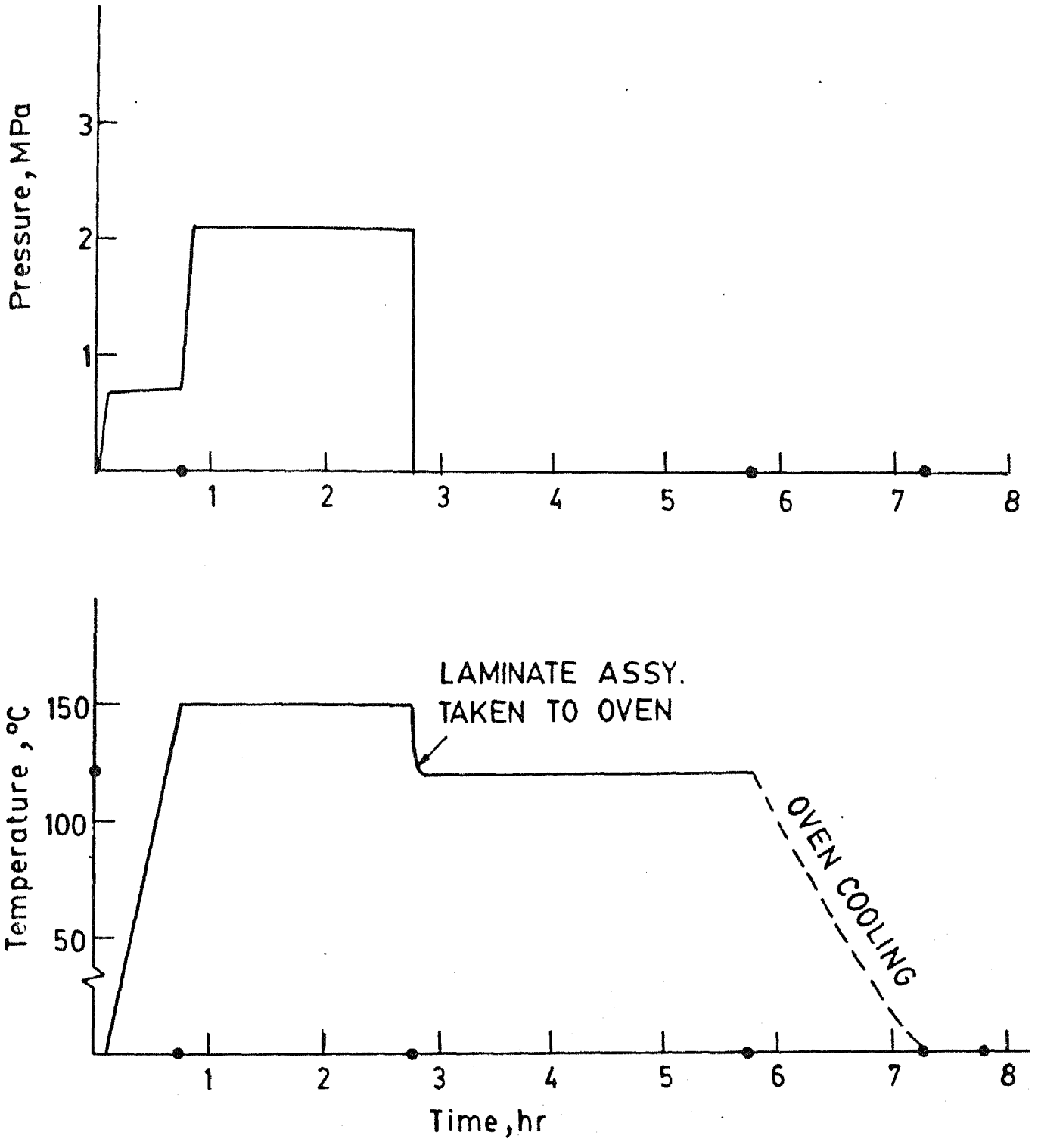

Fig. 3.2 Heat and Pressure Cycle for Laminate Curing

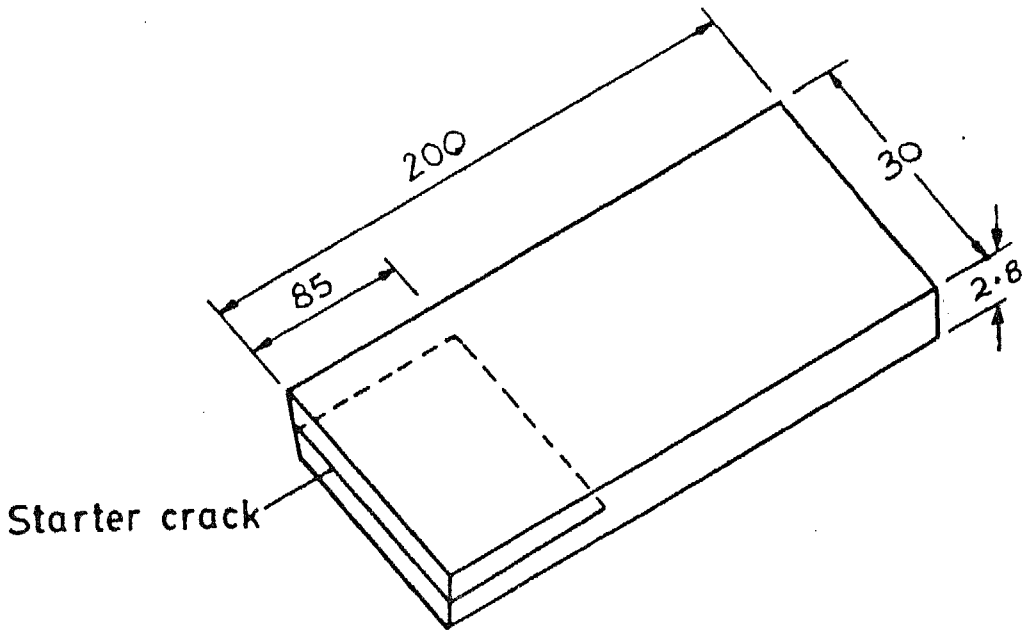

(a)

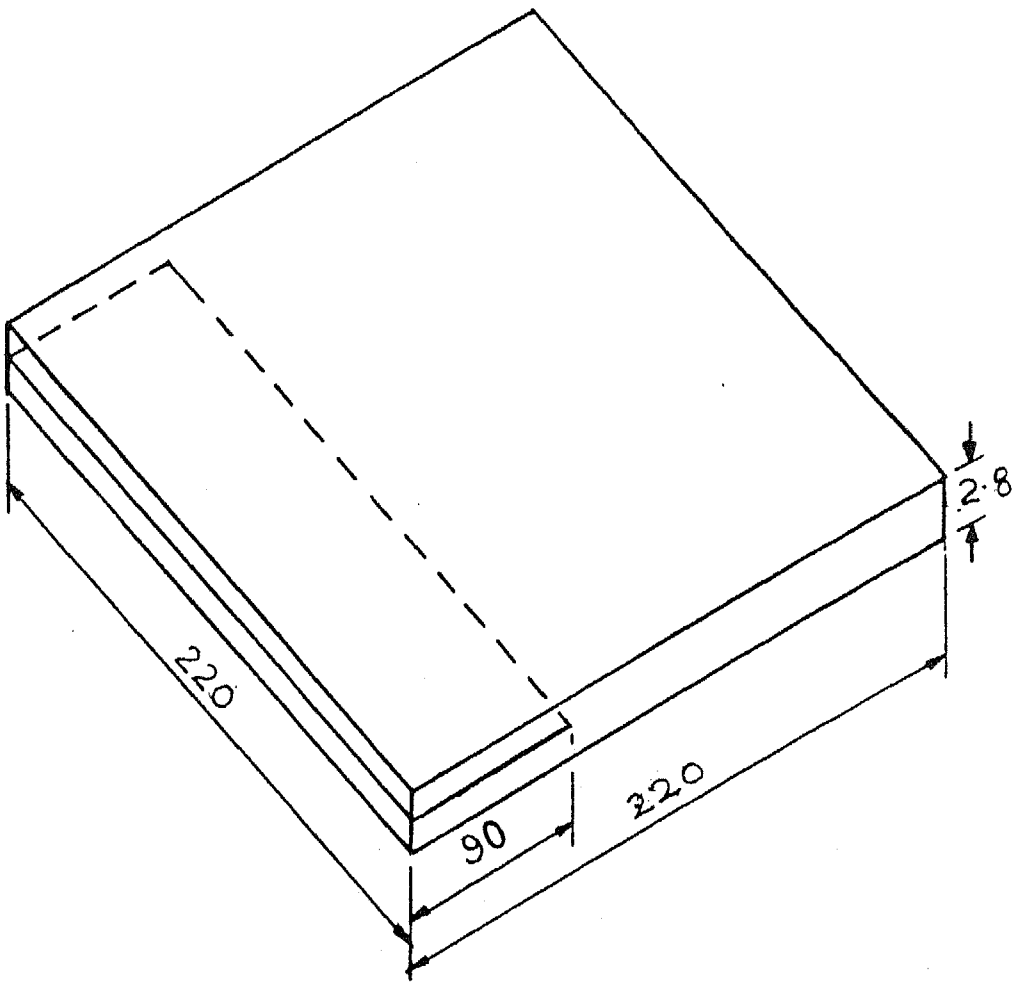

(b)

Fig. 3.3(a) Geometry of DCB Specimen with Artificial Crack

Fig. 3.3(b) Geometry of the Composite Laminate Providing 7 Specimens

steel were glued to its each cantilever. Details of the specimen with hinges are shown in the Fig. 3.4 . On the bottom faces of these hinges and on both sides of the specimen (at one edge) scratches were made for proper bonding. They are bonded together by epoxy (Araldite) at high pressure for six hours. The bond was further allowed to set for 18 hours at room temperature.

3.4 Sharpening of the crack

Crack front was blunt due to the thickness of the teflon sheet used to create the artificial crack during casting. So to get a natural crack front, a wedge made out of 1 mm thick steel blade was inserted between the two cantilevers of the specimen and pushed towards the crack tip under controlled conditions, till it reached the required crack length.

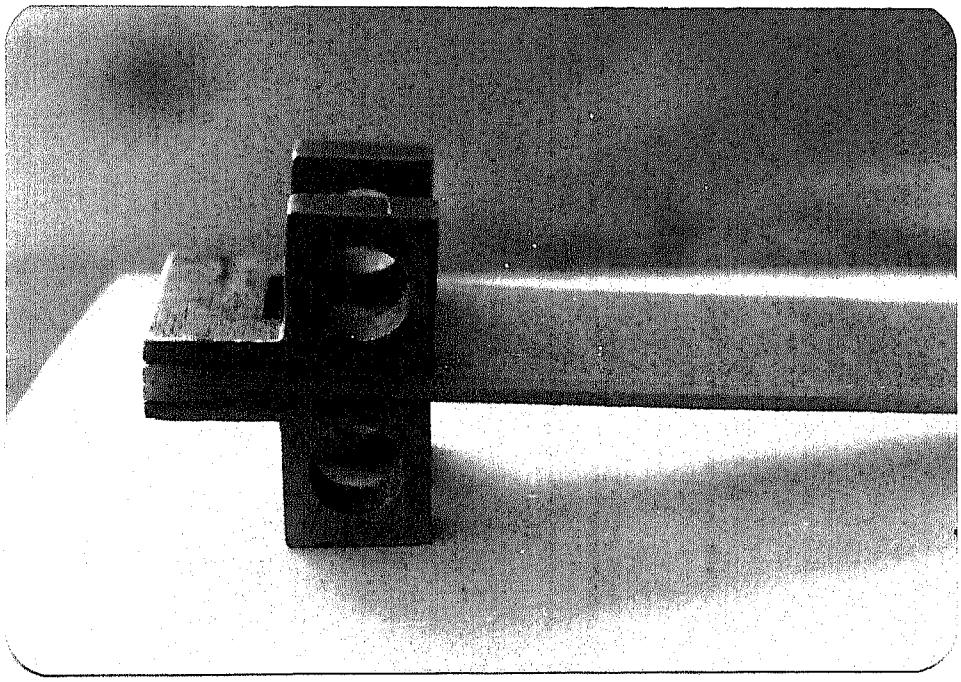

Fig. 3.4 Specimen with Hinges

CHAPTER 4

EXPERIMENTAL TECHNIQUE

4.1 Theoretical Analysis

High strain rate tension test can be conducted by following methods [10].

(i) Conventional load frames.
(ii) Expanding ring test.[11,12]
(iii) Flyer plate and short duration pulse loading.
(iv) Split Hopkinson bar in tension.

In the present work principles of split Hopkinson bar in tension are used. The schematic diagram of the set-up for this experiment is shown in Fig. 4.1. This technique involves the use of a smaller standard type of threaded tension specimen and generation of a tensile pulse directly on the end of the input bar. A mass is impacted directly on the anvil attached to the end of the input bar.

Once the incident pulse of constant amplitude generated by dropping the weight, it travels towards the specimen. On the way it is detected by a strain gauge [13]. Part of the incident pulse is transmitted through the specimen and part of it is reflected. The transmitted pulse is measured by another strain gauge on the transmitted bar. A typical distance - time diagram is shown in Fig. 4.2.

By dropping a weight through a load bar specimen can be loaded by a tinsile pulse of particular width as shown in Fig. 4.2. Incident, reflected and transmitted pulses for the specimen during a time interval can be rcorded.

At the end of the specimen load applied towards the incident bar is given by

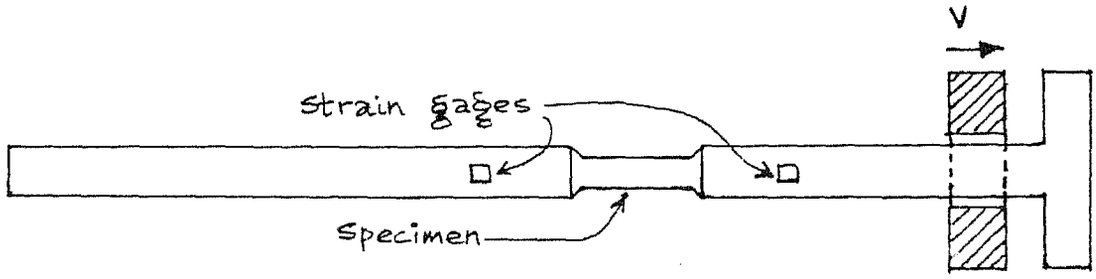

Fig. 4.1 Schematic of the Tension Loading Technique

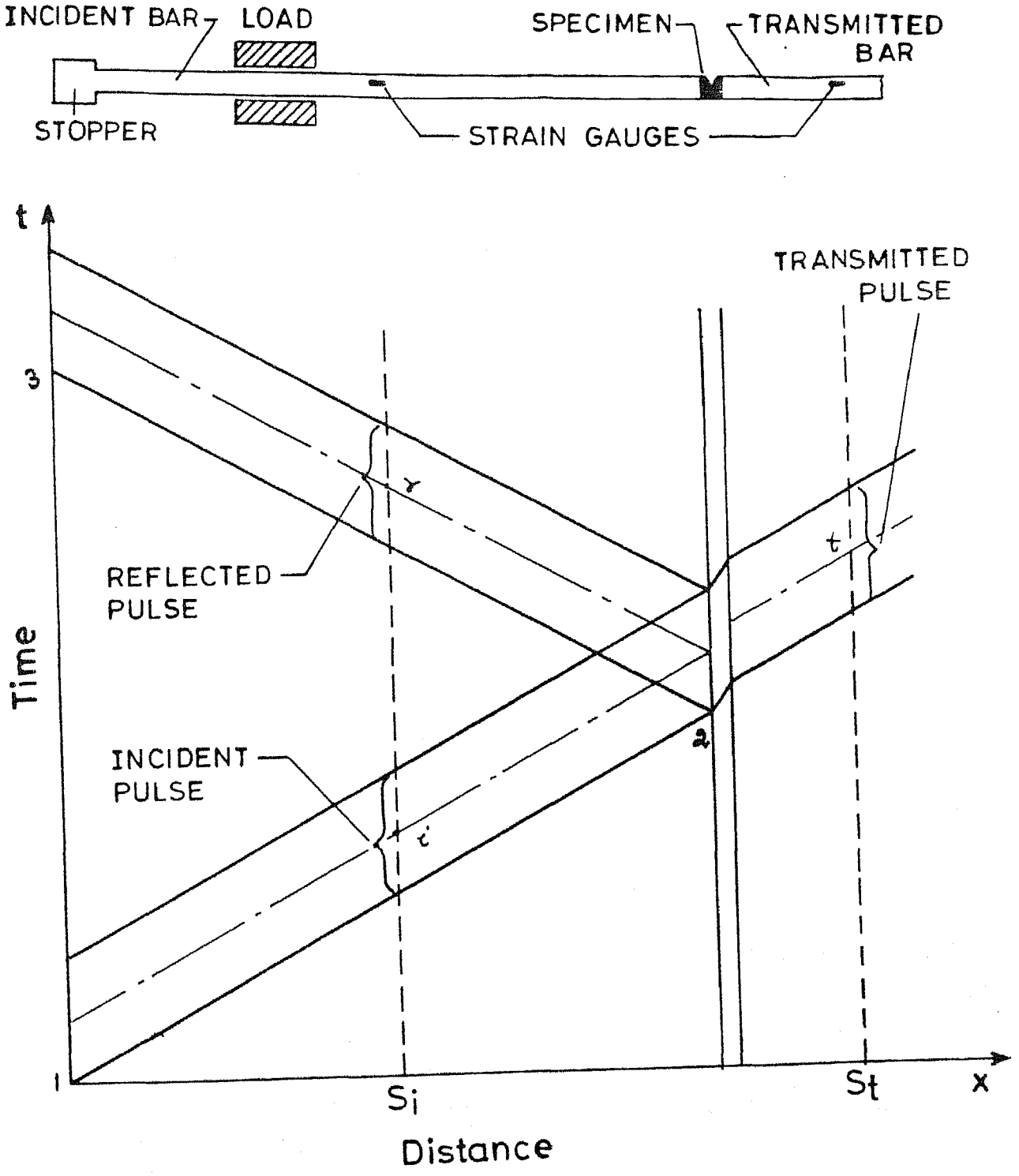

Fig. 4.2 Time Distance (t-x) Diagram

$$P_i = (\sigma_i - \sigma_r) A_i \qquad (4.1)$$

because σ_r is compressive.

Load at the trnsmitted end is given by

$$P_t = \sigma_t A_t \qquad (4.2)$$

The slope of the line 1-2 shown in t-x diagram is 1/c ,where c is velocity of the stress waves in that bar. And along 1-2 the fallowing relation is given by elastic wave theory as

$$\sigma_1 - \rho c v_1 = \sigma_2 - \rho c v_2 \qquad (4.3)$$

Along 2-3 it is given by

$$\sigma_2 + \rho c v_2 = \sigma_3 + \rho c v_3 \qquad (4.4)$$

As a general formula dynmic G_{Ic} is given by

$$G_{Ic} = - \frac{P^2}{2} \frac{dC}{da} \qquad (4.5)$$

where C is complaince of the DCB specimen in which crack is propagating. But C is given as

$$C = \delta / P$$

So from Eq. 4.1 to Eq. 4.5 can be used to find out loads, velocities and hence deflections in some duration of crack propagation to evaluate dynamic G_{Ic}. But later the characterstics of the pulses were not found as simple as in the Fig. 4.2. So detailed analysis of those pulses are discussed in Chapter 5.

4.2 Experimental Set up

The schematic diagram of the experimental set-up is shown in Fig. 4.3. An incident load bar of length 2130 mm and diameter of 10 mm was connected to end of the lower cantilever of a DCB specimen. This incident bar was provided with two teflon guides. At the other end of this bar a stopper of diameter 30 mm and of 33 mm length was connected by a threaded joint. This provides flexibility in changing the dropping weights. The mass of the incident load bar was 1.1 Kg. The transmitted bar of length 1080 mm and the diameter of 12.5 mm was suspended from the roof with a hinge support. At the other end it was provided with a teflon guide which is above the specimen. The load bars were made of mild steel. Overall view of the set-up also given by Fig. 4.4.

'SATYA' Strain Gauges (TRANSENS, Bangalore) with following specifications were used.

Resistance	:	352.0 ± 0.5 ohms.
Gauge Factor	:	2.0
Gauge Length	:	5.0 mm

These strain gauges S_i and S_t were glued at the distances of 1000 mm and 80 mm on the incident and transmitted bars respectively, from the specimen. The cross sectional areas of the incident and transmitted bars at the location of strain gauges were,

$A_i = 64.765 \text{ mm}^2$ and

$A_t = 13.92 \text{ mm}^2$

respectively.

Strain gauges S_i and S_t were connected to separate, identical bridge circuits 1 and 2 respectively by using sealed

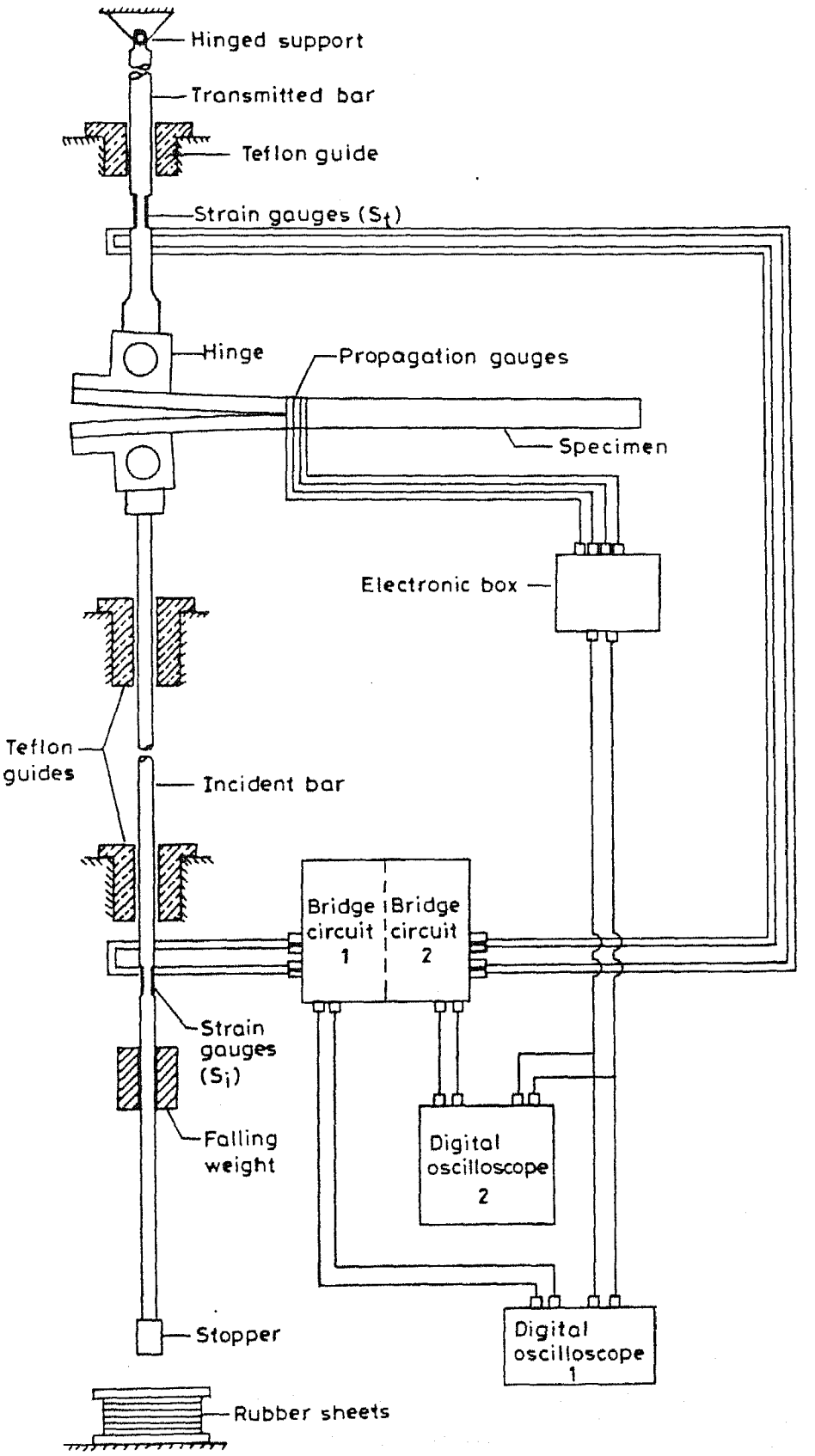

FIg. 4.3 Schematic Diagram of the Experimental Set-up

wires. Bridge circuit used is shown in Fig. 4.6. The out puts from the circuits were connected to two Digital Oscilloscopes (Nicolate 2090 - IIIA).

Crack propagation in the specimen during dynamic loading was monitored by 4 aluminium gauges of thickness 15 microns. First a single piece of aluminium sheet was glued to the specimen, very near to the crack tip. Very narrow strips from the sheet were removed by using a sharpe edged blade thus by making 4 gauges with required spacing (1.5 mm to 2.5 mm) out of that single sheet. The gauges were connected to an electronic box through a junction plate (Fig. 4.5). The electronic box was designed to give some drop in the out put voltage when each of the gauge disconnected from the circuit. It was design to have a very fast response (less than 1 μs). The out put from the electronic box (Fig. 4.7) was connected to both the CRO s in order to synchronize the output signals given by both the strain gauges w.r.t. crack propagation. When crack was propagating gauges broke and electronic box sent signals in a stepped wave form. Duration between these steps and distance between gauges gave crack velocities at corresponding gauges.

The stopper along with the weight was stopped by a bunch of rubber sheets placed on the floor.

For measurement of the loads acting on the specimen, the bridge circuit was calibrated prior to testing. For this purpose following relations were used.

$$\epsilon = - \frac{R_g}{2 S_g (R_g + R_c)}$$

where, S_g is the gauge factor of the strain gauge having resistance R_g. ϵ is the calibration strain corresponds to the voltage diflection on the oscilloscope screen by connecting calibration resistance R_c in the circuit. The loads in the

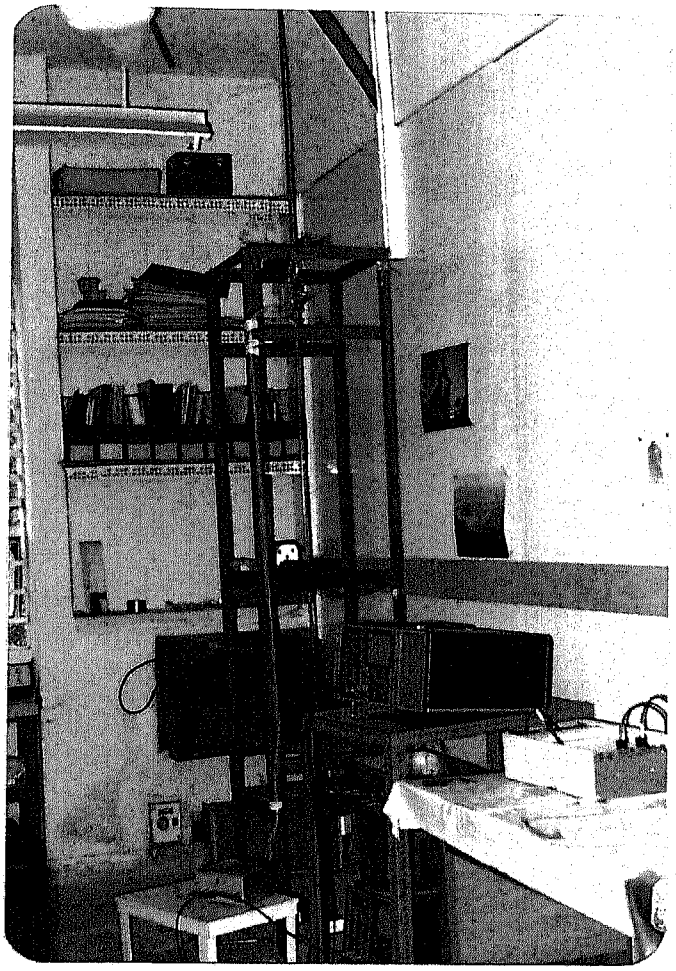

Fig. 4.4 Overall View of the Set-Up.

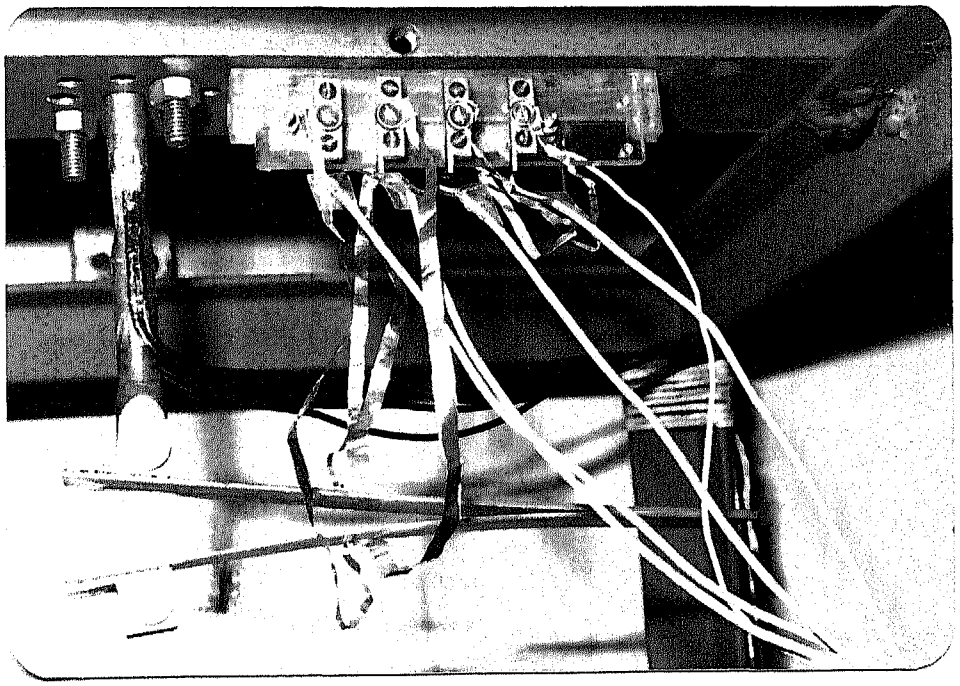

Fig. 4.5 Delaminated Specimen After Dynamic Loading

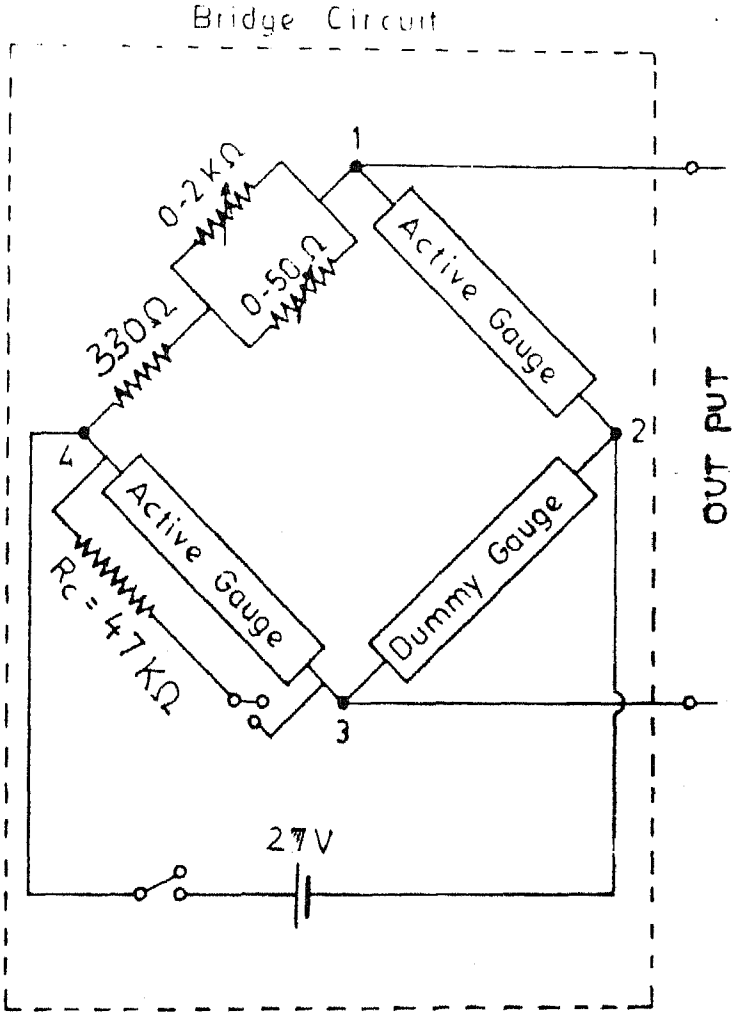

Fig. 4.6 Bridge Circuit

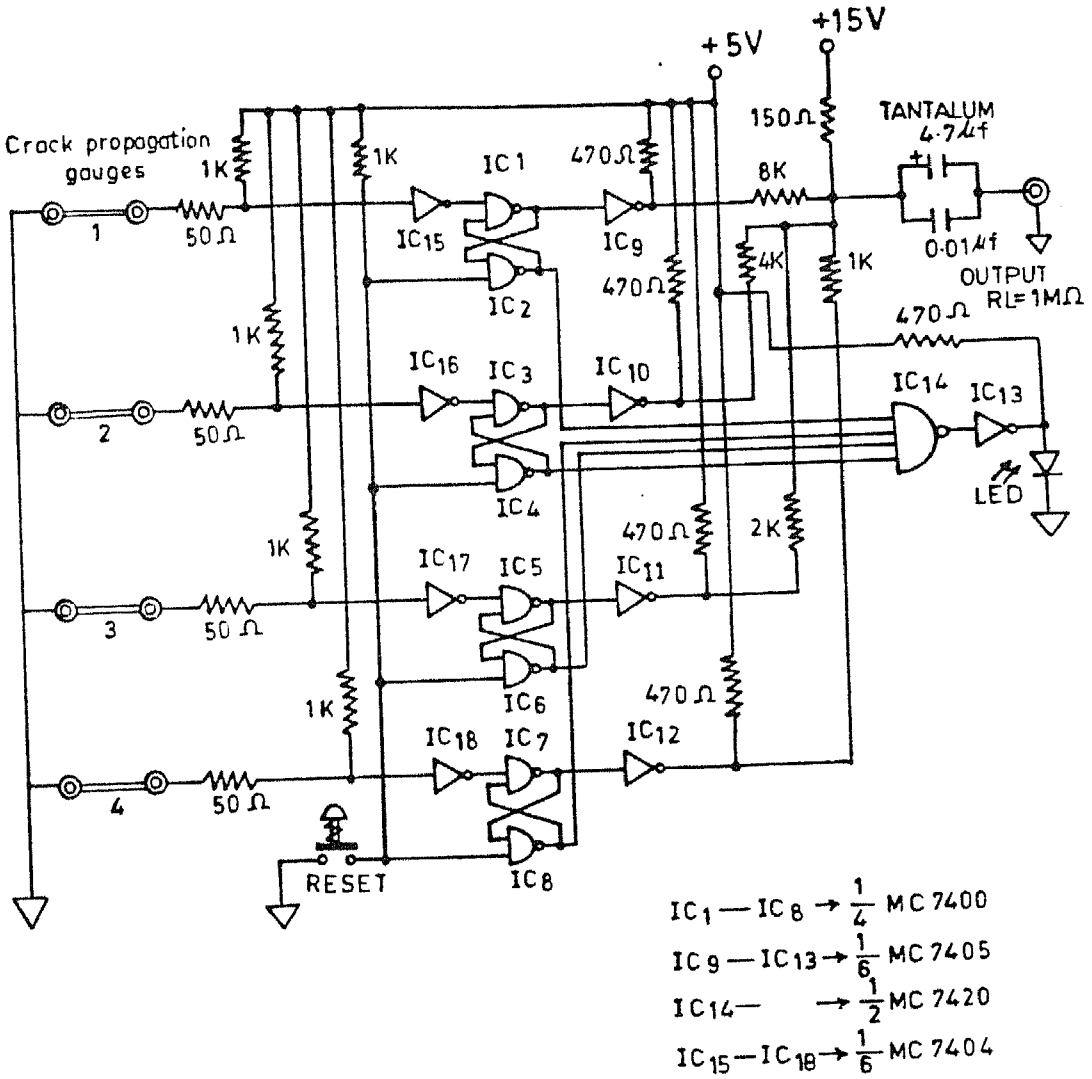

Fig. 4.7 Electronic Box Circuit

incident and transmitted load bars (P_i and P_t respectively) were calculated as

$$P_i = A_i E \epsilon_i \qquad \text{and}$$

$$P_t = A_t E \epsilon_t$$

where E is the Young's Modulus of the load bars which is 207 GPa.

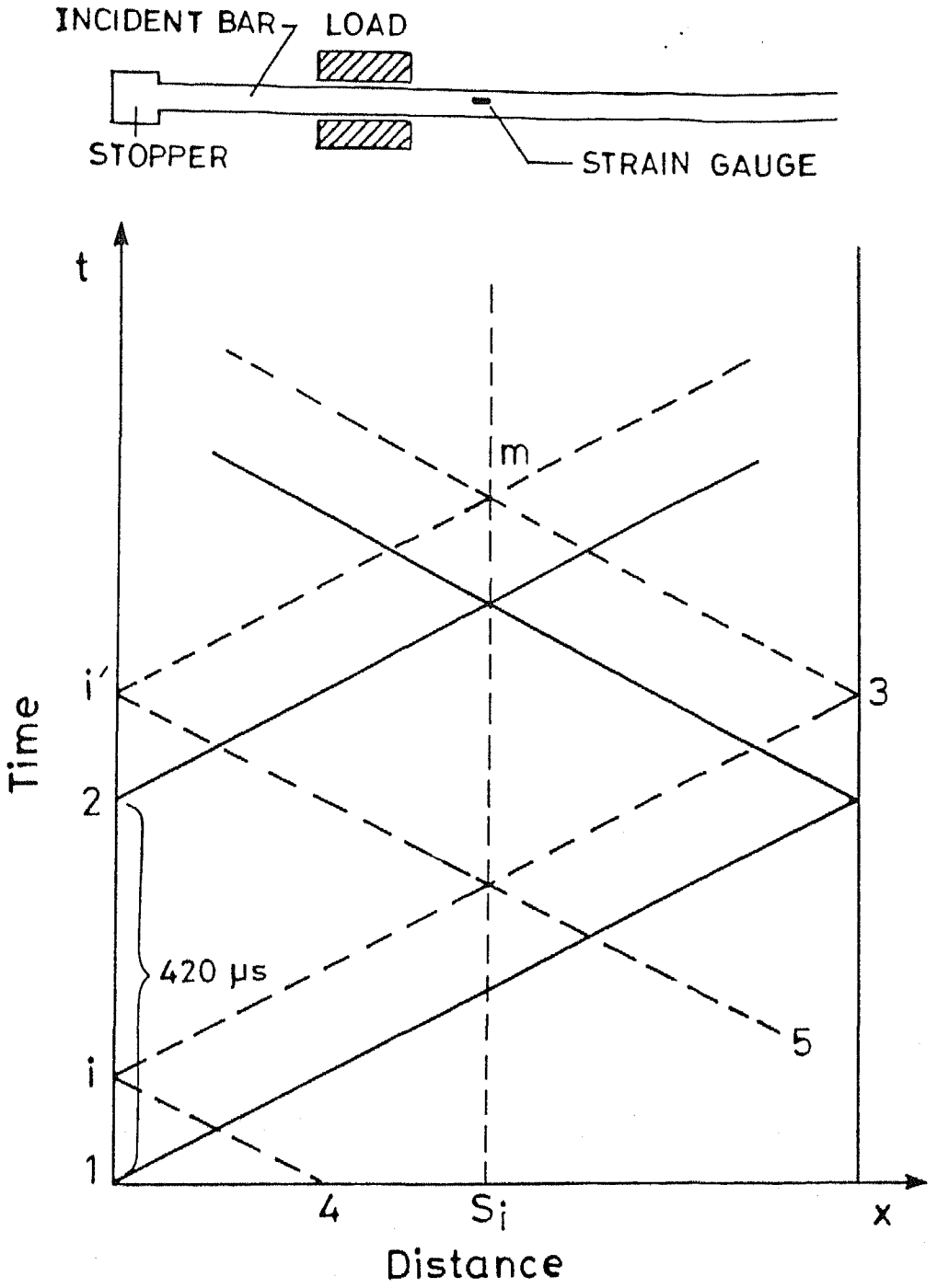

Fig. 5.1 Time-displacement (t-x) Diagram

when the incident pulse arrived at the interface. Consequently, the tensile incident pulse was reflected into the load bar as compressive pulse of same magnitude and character. This helps us in determining the tail of the incident pulse. Fig. 5.1 shows the t-x diagram of the experiment.

At the point 1 (t=Ø) tensile pulse started and after some time it reached strain gauge S_i. The point 2 represents the time at which the incident pulse started mixing with the reflected pulse. We are interested in calculating the pulse after point 2. An incident pulse started from point i was reflected from point 3 and mixed with the incident pulse started from i', at point m.

σ_i (between 1 & 2) and σ_m (after 2) were measured.

is mass density of the load bars (78ØØ Kg/m^3) and c is the velocity of the stress waves in the load bar material (515Ø m/s). From the elastic wave propogation theory following analysis is made.

Along i' - m,

$$\sigma_{i'} - \rho c v_{i'} = \sigma_m - \rho c v_m \qquad (5.1)$$

Along 3 - m,

$$\sigma_m + \rho c v_m = \sigma_3 + \rho c v_3 \qquad (5.2)$$

But $\sigma_3 = Ø$ since the end of the bar is free at point 3.

Along i - 3,

$$\sigma_3 - \rho c v_3 = \sigma_i - \rho c v_i \qquad (5.3)$$

But along i - 4,

$$\sigma_i + \rho c v_i = \sigma_4 + \rho c v_4 \qquad (5.4)$$

CHAPTER 5

RESULTS AND DISCUSSIONS

The lower cantilever of the DCB specimen was loaded by dropping a weight (3.8 kg) from a height of one meter. The incident pulse in the lower bar was recorded by the strain gauge (S_i). The pulse was reflected from the end of the lower cantilever which was again recorded by the strain gauge. The transmitted pulse was recorded by the strain gauge (S_t) of the transmitted load bar. The load and velocity were obtained of the lower cantilever from the records of the incident and reflected pulses in the incident load bar by applying one-dimensional wave theory for an elastic bar. Similarly, the transmitted pulse provided the load and the velocity of the upper cantilever.

5.1 Incident Pulse

Contrary to the earlier expectations, the reflected pulse could not be recorded separately as, by the time the reflected pulse arrived at the strain gauge (S_i) the incident pulse did not die out. The energy of the dropping weight was so high that the duration was much longer than expected. Therefore, after 420 μs, which corresponds to twice the travel time of the pulse between the strain gauge and the tip of the cantilever, the two pulses were superimposed. It was essential to separate out the reflected pulse from the tail of the incident pulse.

A separate experiment was conducted by replacing the specimen with a thin cotton thread of diameter 0.6 mm.

The acoustic impedance of the cotton thread was about 16% of steel load bar and its area was only 0.36 % of the bar. The net impedance mismatching was only about 1600 : 1 and therefore, it can be assumed that the cotton thread did not generate any load

But at $t = \emptyset$, σ_4 and v_4, are zero hence Eq. 5.4 gives,

$$v_i = - \sigma_i / \rho c$$

Substituting this in Eq. 5.3 gives,

$$- \rho c v_3 = \sigma_i + \sigma_i$$

i.e. $$v_3 = - 2\sigma_i / \rho c$$

Substituting v_3 in Eq. 5.2 gives,

$$\sigma_m + \rho c v_m = c(-2\sigma_i / c) = - 2\sigma_i$$

Therefore, $$v_m = -(2\sigma_i + \sigma_m)/\rho c$$

Substituting this in Eq.5.1 gives,

$$\sigma_i' + \sigma_i' = \sigma_m + \rho c(2\sigma_i + \sigma_m)/\rho c$$

Therefore, $$\sigma_i' = \sigma_m + \sigma_i$$

Using the above equation incident pulse after point 2 was processed. To process the data of Fig. 5.2, the ripples in the incident and the mixed pulses were smoothened out by fitting a mean curve approximately which balances the areas of both sides of the curve fitted. Fig. 5.3 provided processed incident pulse upto 840 μs.

5.2 Dynamic Crack Propagation in GFRP

Three experiments were conducted with the same drop weight and drop height. The location of propagation gauge with respect to the crack tip could not be measured accurately as the crack tip was not straight.

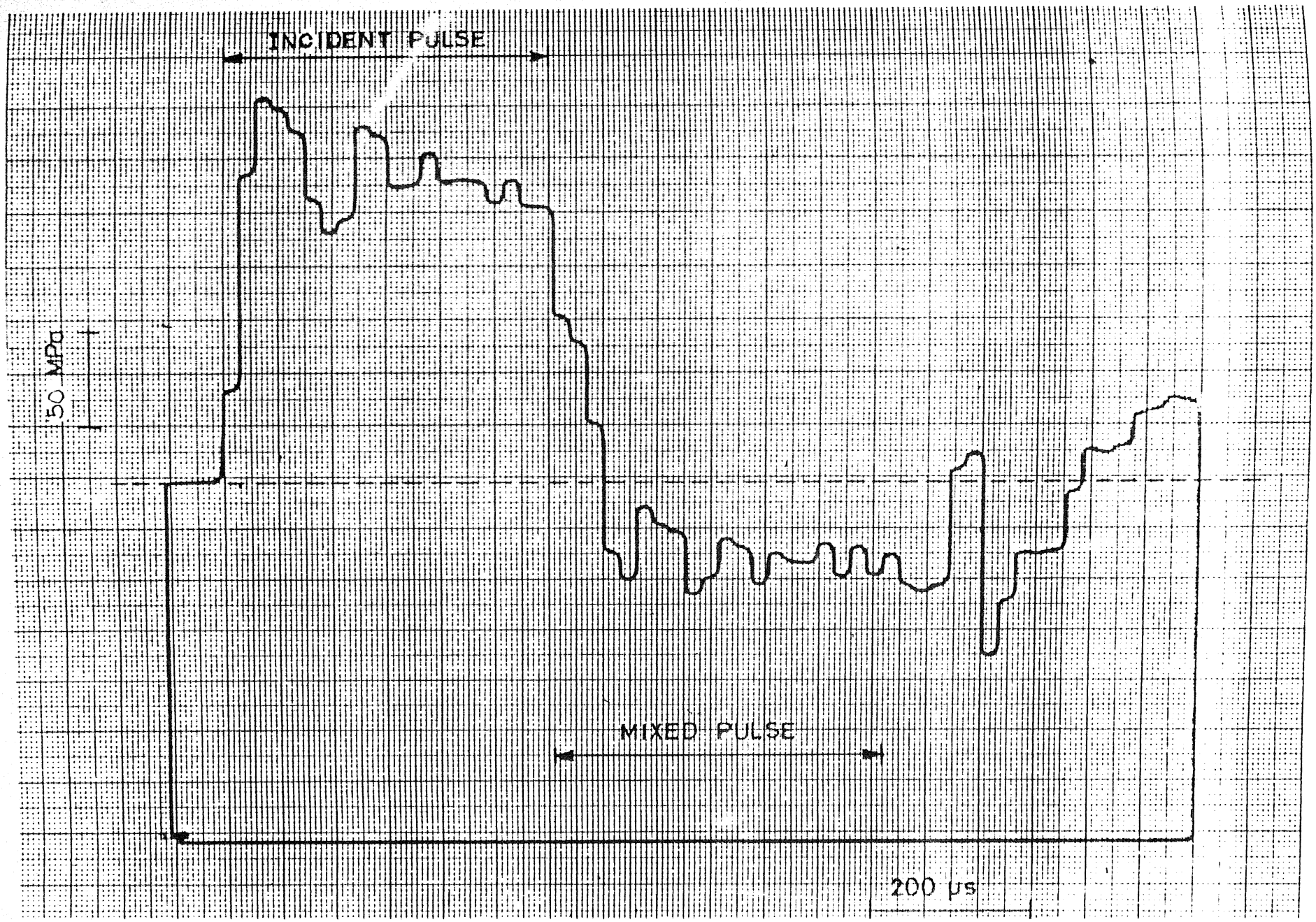

Fig. 5.2 Transient Stress Record at Strain Gauge S_1
(suspended by thread)

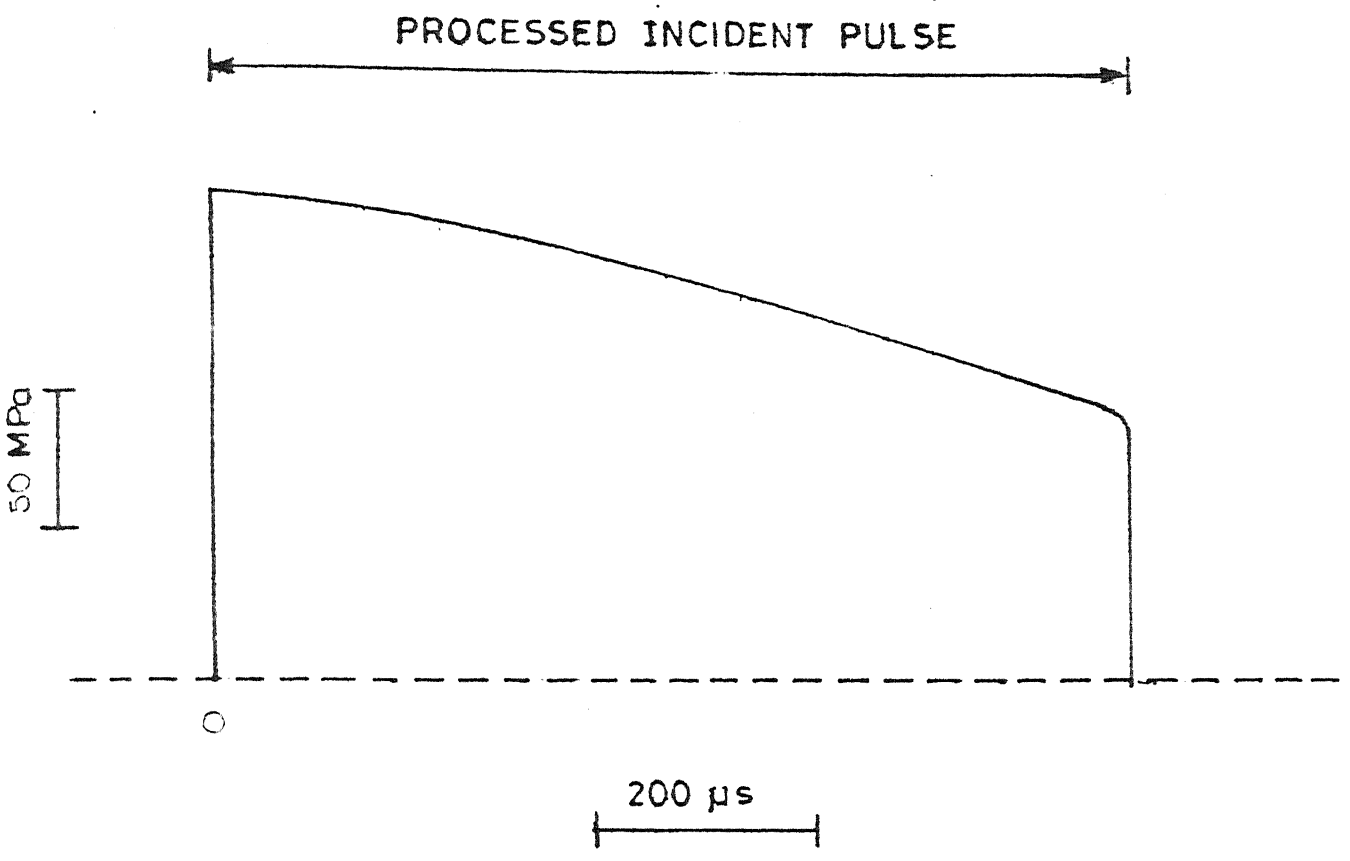

Fig. 5.3 Processed Incident Pulse

Fig. 5.4 shows the strain gauge record in the incident bar. The reflected pulse was superimposed on the tail of the incident pulse. Since the pulses were not separated, this required an analysis slightly different from what was presented in Chap. 4. Fig. 5.6 shows the t-x diagram for the analysis.

We are interested in finding out the velocity and the stress at point 3. σ_i and σ_m during 420 μs were found out from the X-Y plot.

Along i - 3,

$$\sigma_3 - \rho c v_3 = \sigma_i - \rho c v_i \tag{5.5}$$

Along 3 - m,

$$\sigma_3 + \rho c v_3 = \sigma_m + \rho c v_m \tag{5.6}$$

But along i - 4,

$$\sigma_i + \rho c v_i = \sigma_4 + \rho c v_4$$

Since σ_4 and v_4 are zero at t = Ø, we get

$$v_i = - \sigma_o/\rho c \tag{5.7}$$

Along i' - m,

$$\sigma_{i'} - \rho c v_{i'} = \sigma_m - \rho c v_m \tag{5.8}$$

But along i' - 5,

$$\sigma_i + \rho c v_{i'} = \sigma_5 + \rho c v_5$$

Since σ_5 and v_5 are zero at the instant of recording the pulses.

$$v_{i'} = - \sigma_{i'}/\rho c \tag{5.9}$$

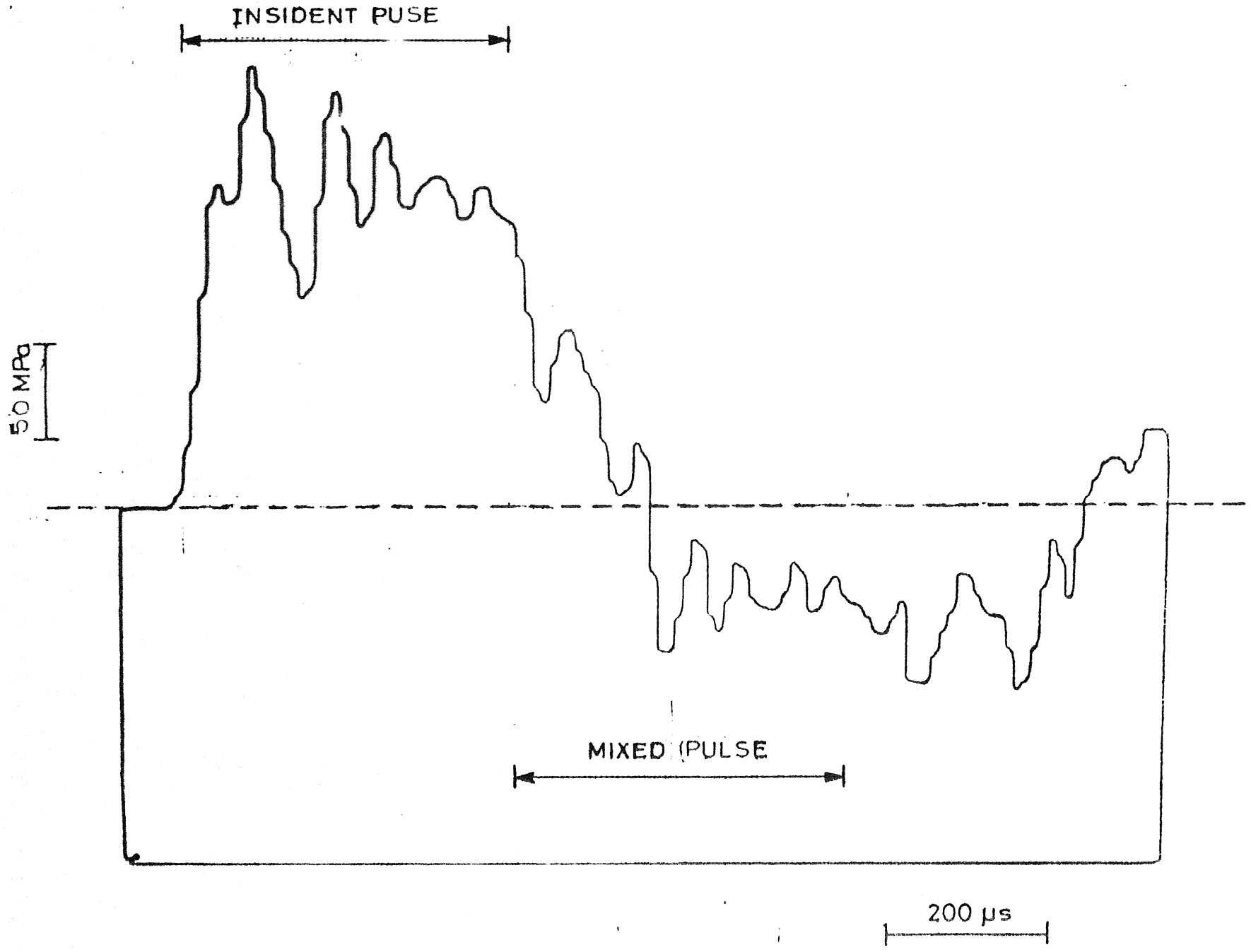

Fig. 5.4 Transient Stress Record of Exp. 1 at Strain Gauge S_1

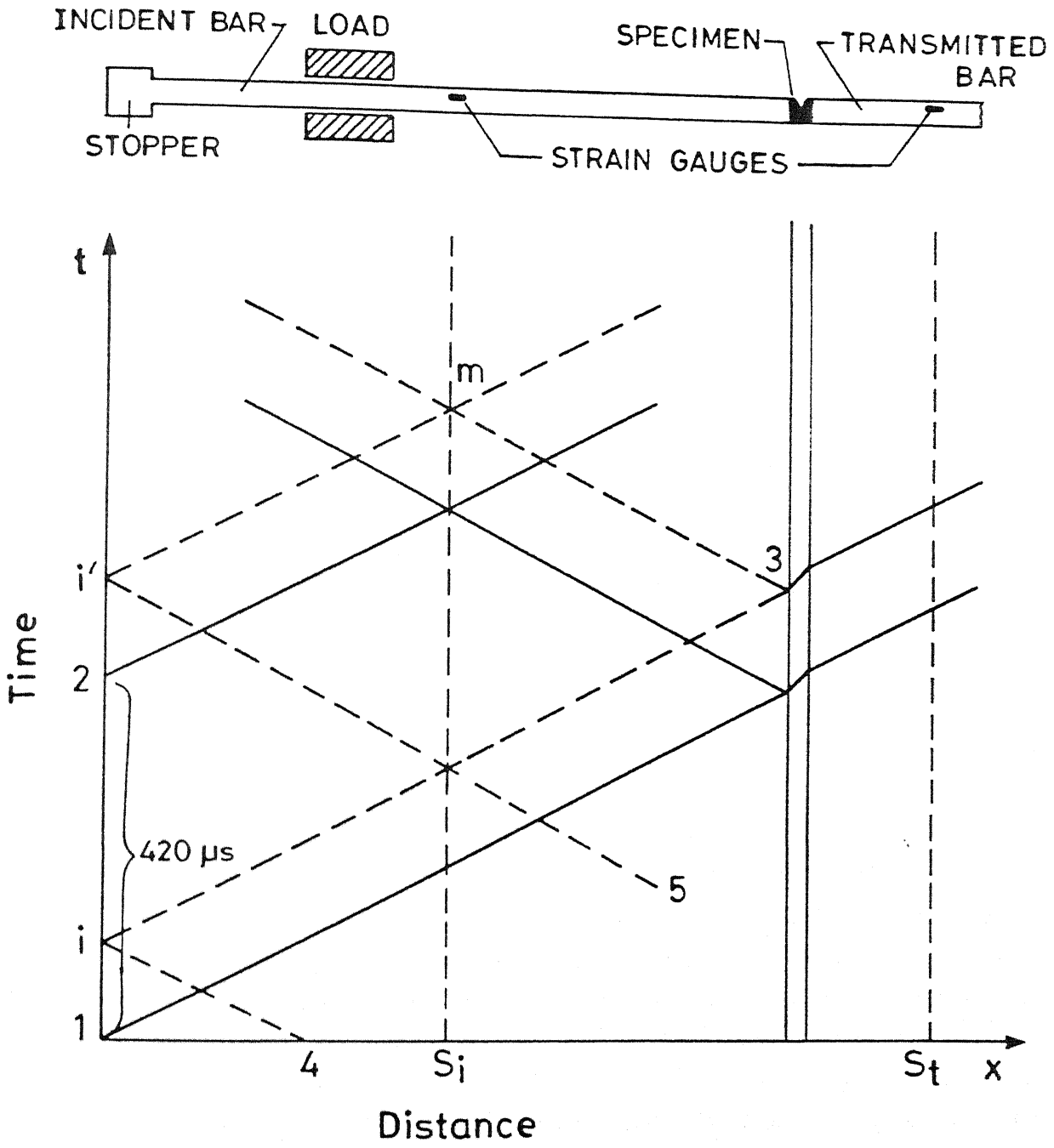

Fig. 5.6 Time - Distance (t-x) Diagram (Loaded Specimen)

Substituting Eq. 5.9 in Eq.5.8 we get,

$$v_m = (\sigma_m - 2\sigma_i')/\rho c \qquad (5.10)$$

Substituting Eq.5.7 in Eq. 5.5 and Eq. 5.10 in Eq. 5.6 we get,

$$\sigma_3 + \rho c v_3 = 2\sigma_m - 2\sigma_i'$$

$$\sigma_3 - \rho c v_3 = 2\sigma_i$$

Solving the 2 Eqs. for the two unknowns σ_3 and v_3, we get

$$\sigma_3 = \sigma_m + \sigma_i - \sigma_i'$$

$$v_3 = (\sigma_m - \sigma_i' - \sigma_i)/\rho c$$

Data of the X-Y plot was processed in the same way as in the previous case.

The load on the tip of the cantilever becomes,

$$P_i = (\sigma_m + \sigma_i - \sigma_i') A_i$$

Where A_i is the cross sectional area of the load bar at the location of the strain gauge S_i

The crack velocity was determined from the voltage drops (Fig. 5.5) corresponding to the snapping of propagation gauges by the advancing crack. The crack velocity was 92m/s. It was measured 1690 μs after the head of the incident pulse reached the tip of the lower cantilever. In all the three experiments in this study, this time t_p, (The instant at which the velocity measurement with respect to the beginning of the loading at the cantilever tip) signifies after how much later the crack velocity was measured. In fact, at time t_p, the crack acquires a high velocity.

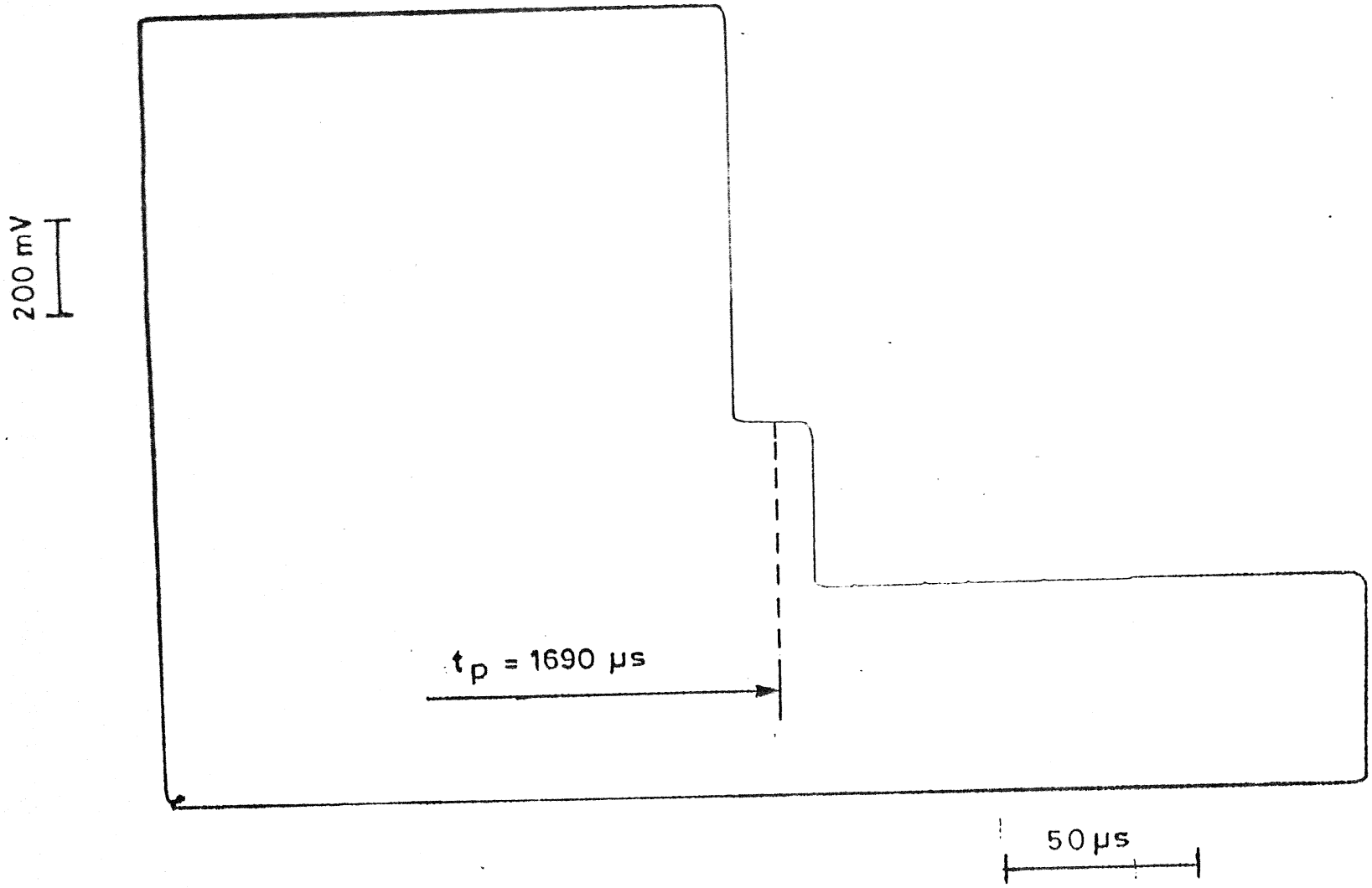

Fig. 5.5 Crack Propagation Record of Exp. 1

The load and the velocity plots of the cantilever tip w.r.t. time are shown in Fig. 5.7 and 5.8 respectively. The load increases to a high value of 8.Ø1 KN, in a very short time (35 μs) and it dies out in about 27Ø μs. On the other hand, the velocity increases rapidly in the beginning and reaches a maxima of 8.1 m/s at 27Ø μs. Then after it decreases gradually. The specimen provides resistance to the incident load bar only for 27Ø μs and thereafter, the end of the load bar moves freely like it did in case of the experiment with the thread. The velocity of the end decreases gradually because the incident pulse tapers down with time. In other words, after 27Ø μs, the incident bar did not measure any load between the bar and the specimen. Most probably, there was some load but was outside the reach of the experimental setup.

The energy release rate G_{Ic} can be determined by,

$$G_{Ic} = - \frac{P^2}{2b} \frac{dC}{da} \qquad (5.11)$$

Where, b is the width of the specimen and the compliance of the lower cantilever beam is given by

$$C = \delta / P$$

δ is determined by integrating the velocity numerically. At time t_p the load P was very small. If this is considered to be the case of the constant loading,

$$\frac{dC}{da} = \frac{1}{Pb} \frac{d\delta}{da}$$

Substituting in Eq. 5.11, one obtains

$$G_{Ic} = - \frac{P}{b} \frac{d\delta}{da} \qquad (5.12)$$

Also, $d\delta/da$ can be expressed in terms of velocities as,

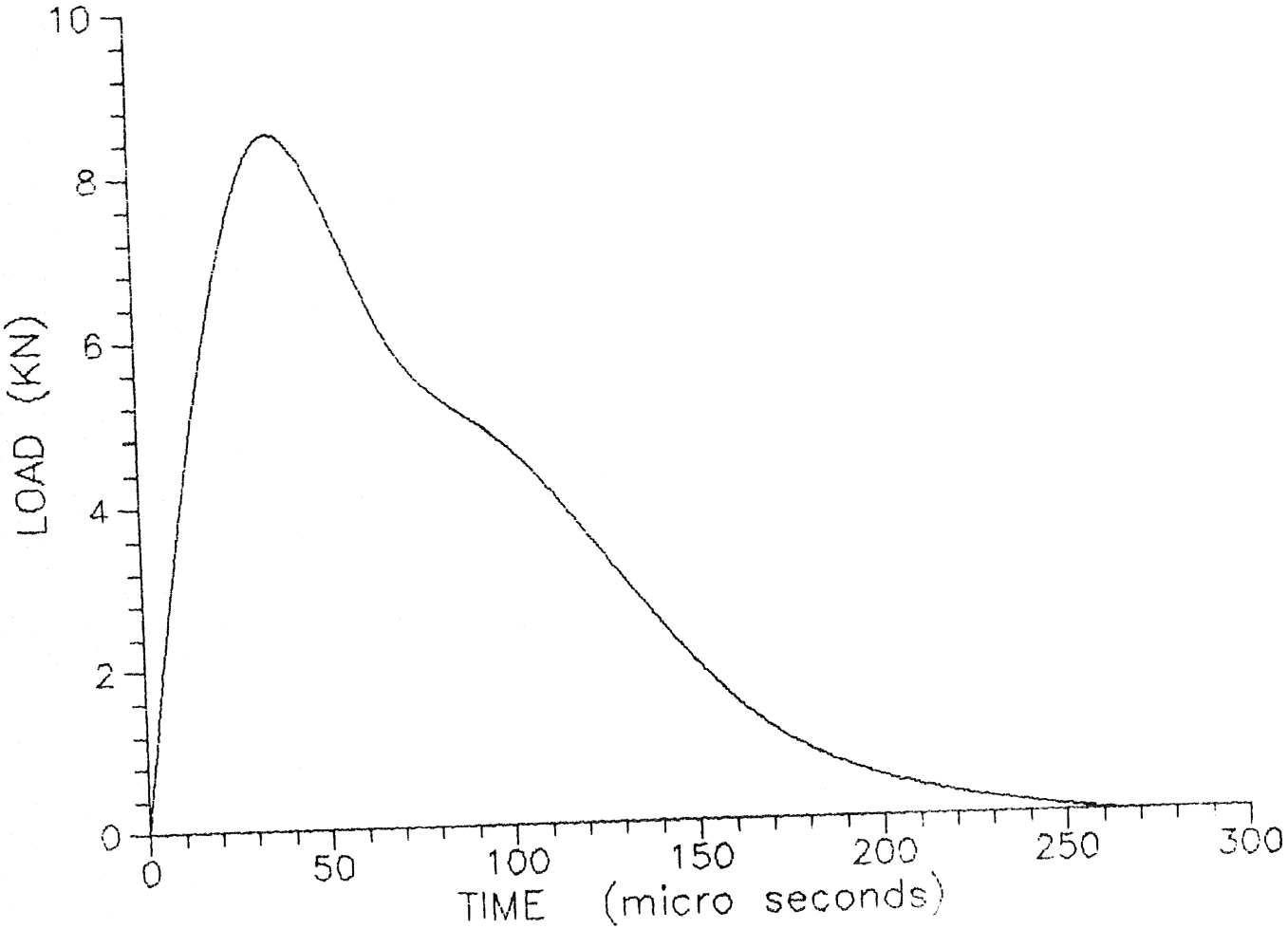

Fig. 5.7 Load - Time (p-t) Diagram of Exp. 1

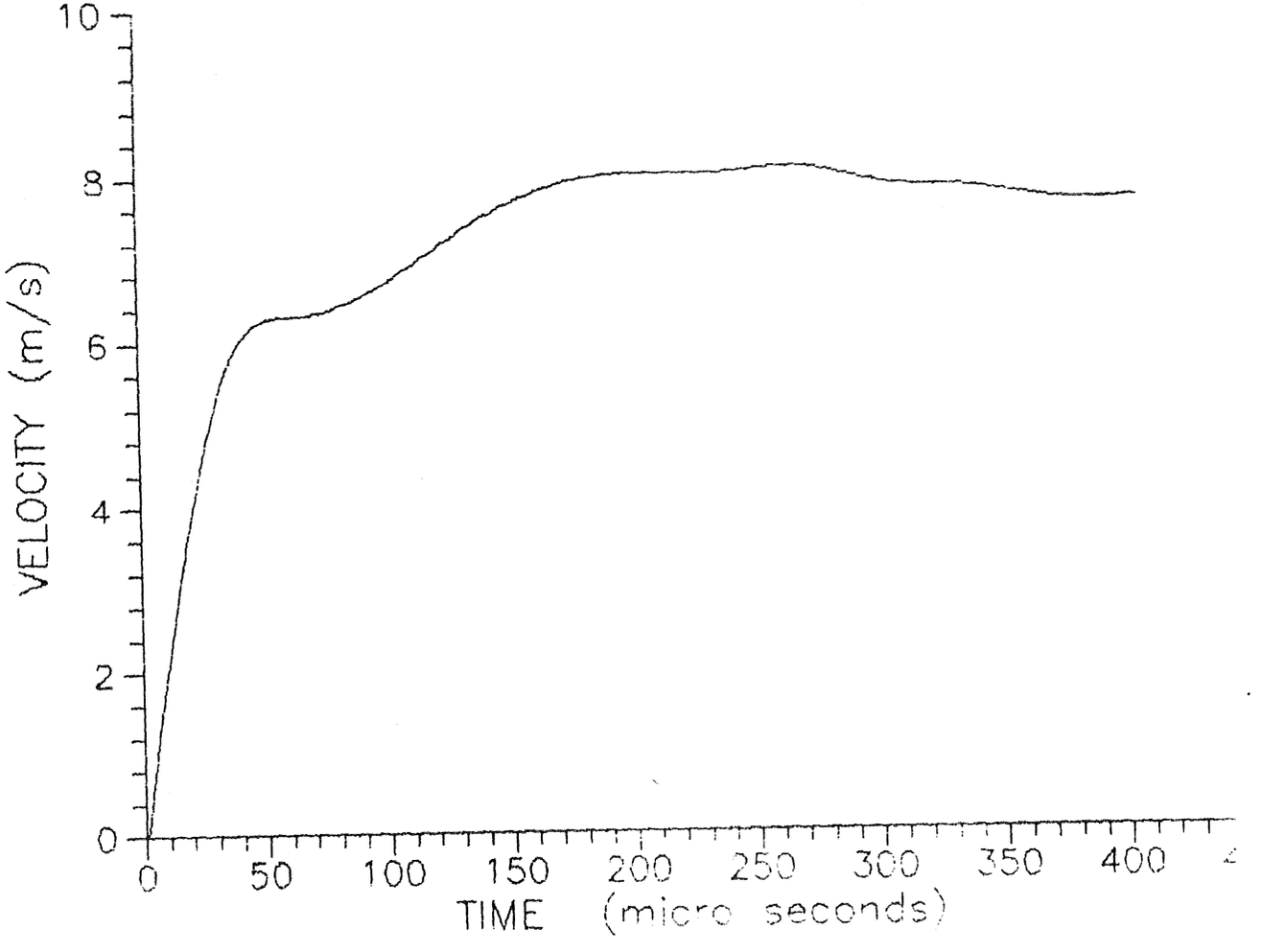

Fig. 5.8 Velocity - Time (v-t) Diagram of Exp. 1

$$\frac{d\delta}{da} = \frac{d\delta/dt}{da/dt} = \frac{v}{\dot{a}}$$

Where $\dot{a}$ is the crack velocity. Then the Eq. 5.12 changes to

$$G_{Ic} = -\frac{P}{b}\frac{v}{\dot{a}}$$

In this experiment at time t_p, v is less than 8.Ø5 m/s and $\dot{a}$ is 92 m/s, providing $v/\dot{a} < Ø.ØØ9$

Thus,

$$G_{Ic} < Ø.ØØ9\ P/b$$

Since P is so small that it was not measured by the experiment, G_{Ic} is extremely low at the runaway speed of the crack. This suggests that the crack was running in a brittle manner, requiring very small energy. After it acquired the high speed. Probably, as the crack advanced, it did not cause much of a damage around the crack tip and it required energy only to overcome the surface energies of solids. Typically, the surface energy of a solid is of the order of 1 J/m^2, which is much smaller than the quasistatic G_{Ic} of 7ØØ J/m^2.

In the early state of crack propagation, work was done on the specimen but G_{Ic} was not evaluated by Eq. 5.11 because dC/da was not monitored by the propagation gauges. However, large amount of energy was required to make the crack move at very high speeds. It was determined by finding out the external work done on the specimen, W_{ext} as,

$$W_{ext} = \int Pv\ dt$$

This Critical Crack Tip Energy (CCTE) per unit length of the crack tip was required to accelerate the crack to the high speed. The value of CCTE for this experiment was 17Ø.2 J/m.

The very low value of G_{Ic} at high speeds may explain the large damage observed in a panel impacted by a foreign body. Crack velocities as high as 300 m/s have been observed through high speed cameras on impacted panels [14].

The strain gauge and crack propagation records for Exp. 2 are shown in Fig. 5.9 for the lower cantilever beam. Fig. 5.10 shows feeble transmitted pulses recorded by the strain gauge S_t. So range of maximum value of P_u is shown by dotted linesin P-t diagram(Fig. 5.11). Because transmitted stress pulses were very small it was assumed that loads and velocities of the upper cantilever tip were hardly contributig in the external work done on the specimen. In these dynamic experiments the lower cantilever was loaded by the inertia of the specimen. Velocity - time relation for Exp. 2 is given in Fig. 5.12. In Exp. 3, four propagation gauges were used. The first propagation gauge was found to be bonded slightly before the crack tip and therefore, shows small duration between the first two propagation gauges (Fig. 5.13). The crack accelerated between the second and the third and finally acquires high velocity monitored by the fourth gauge.

The load and the velocity for all the experiments are presented in Fig. 5.14 and 5.15 respectively. The results of the three experiments are provided in Table 5.1. The table shows consistent value of CCTE (with 2.1 %). The small value of t_p in Exp. 2, is not understood.

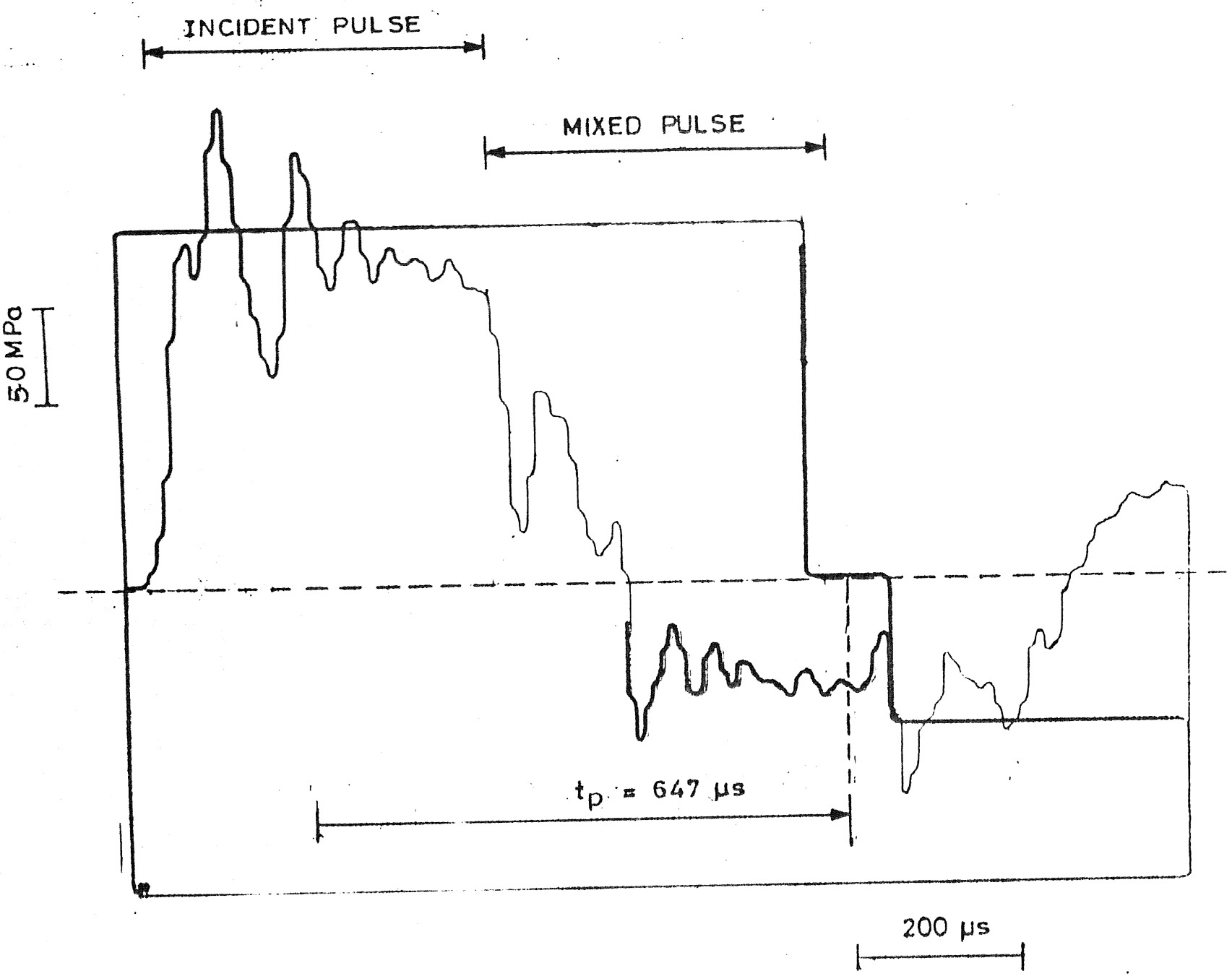

Fig. 5.9 Transient Stress and Crack Propagation Record of Exp. 2 at Strain Gauge S_1

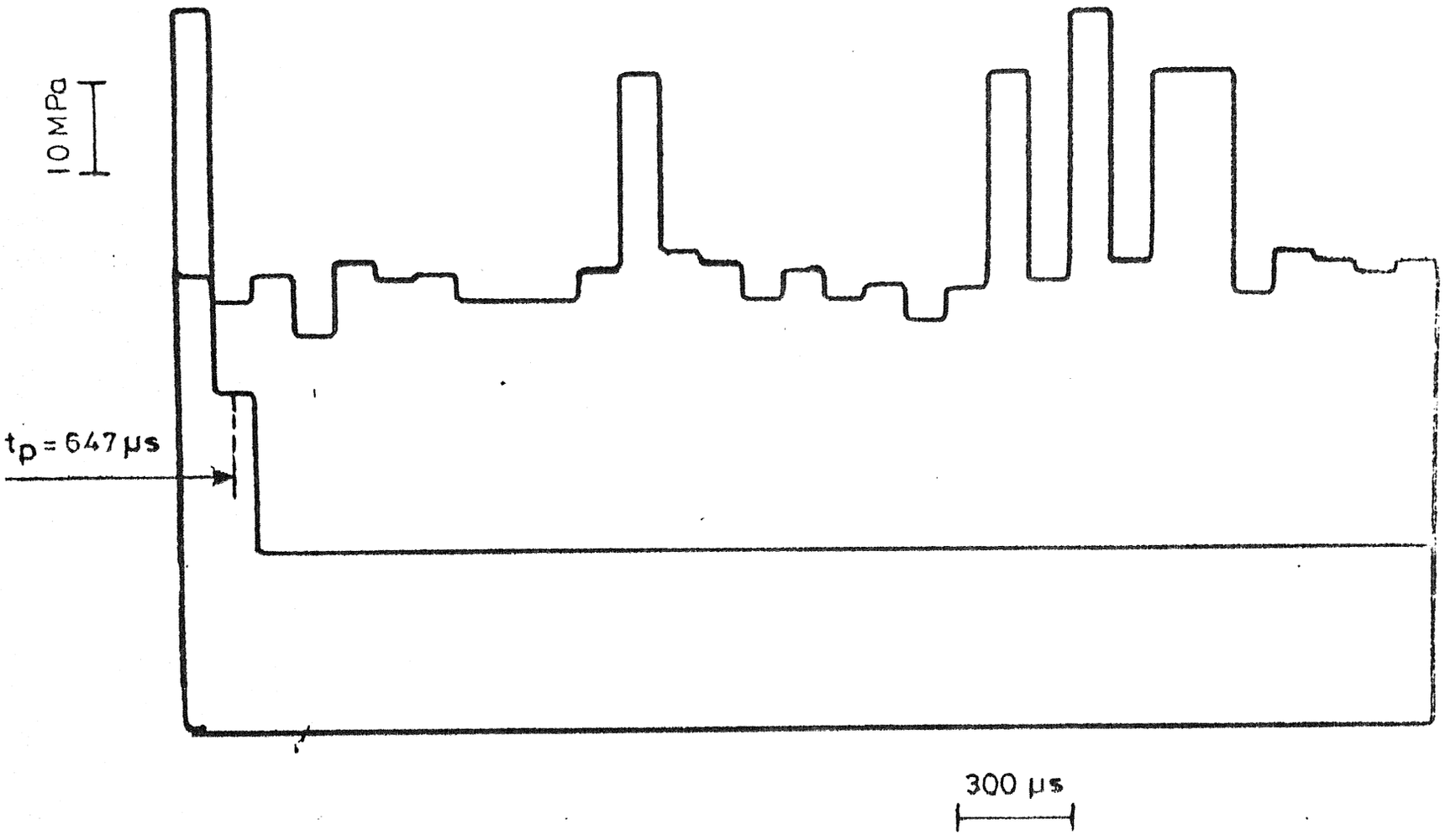

Fig. 5.10 Transient Stress and Crack Propagation Record of Exp. 2 at Strain Gauge S_t

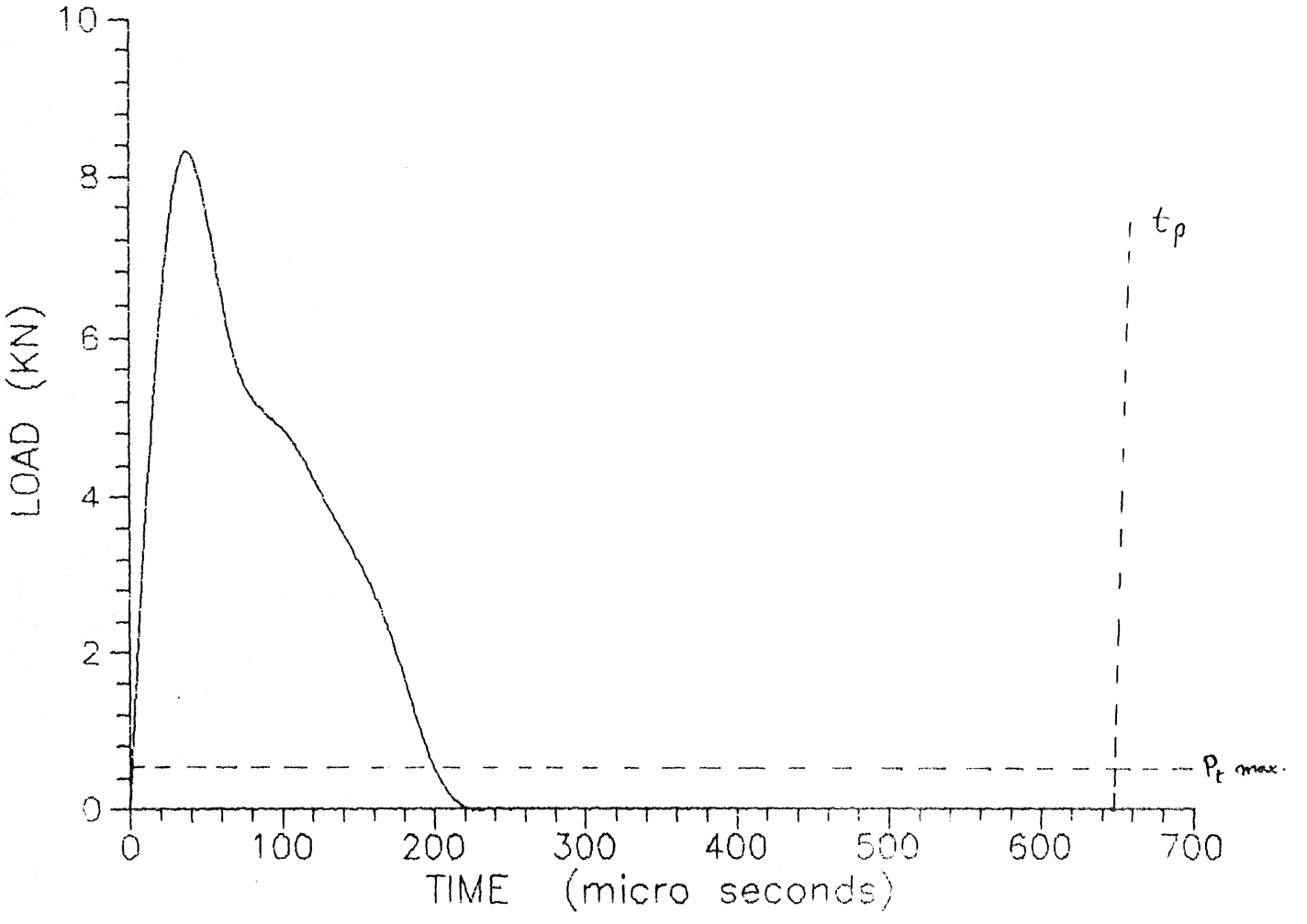

Fig. 5.11 Load - Time (p-t) Diagram of Exp. 2

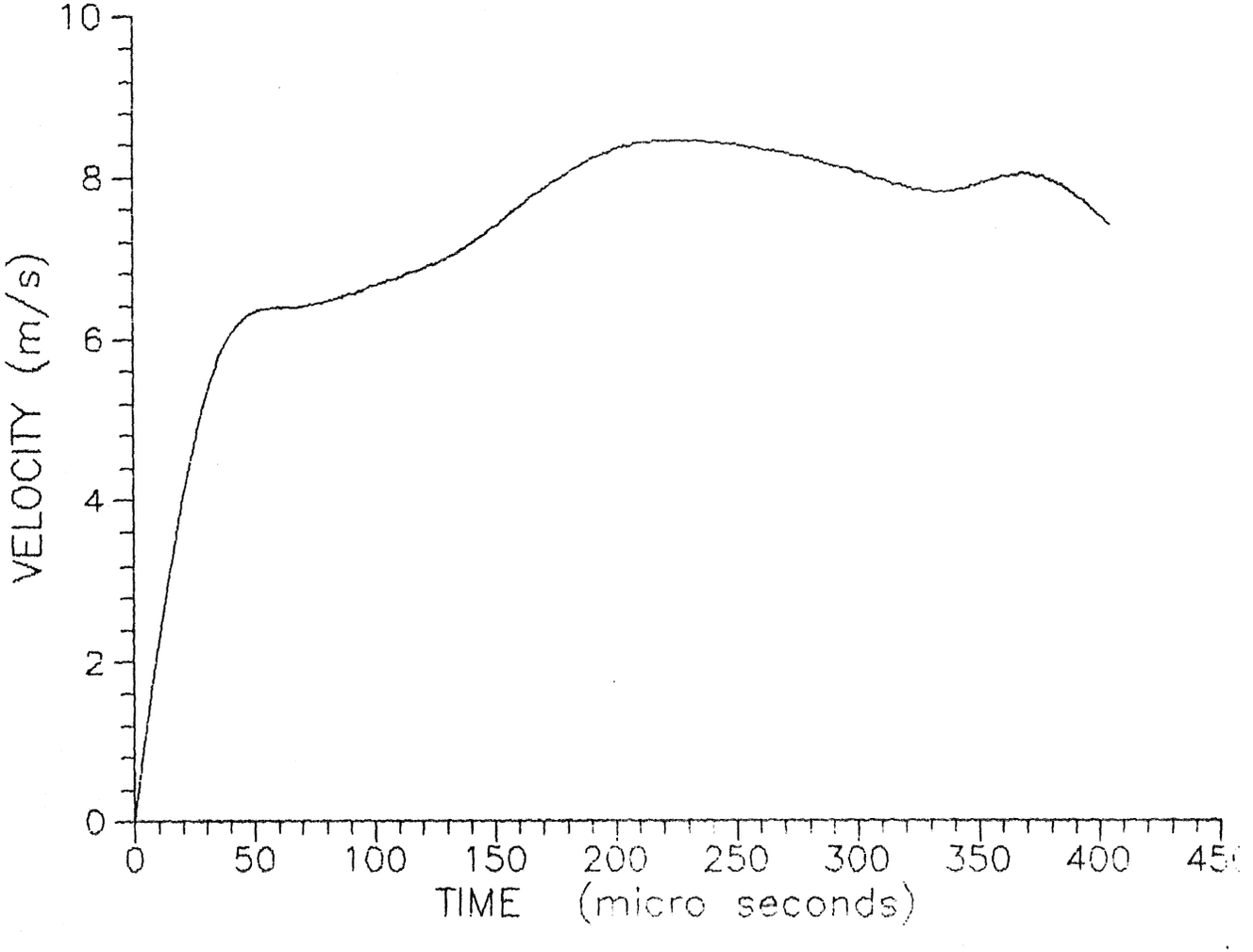

Fig. 5.12 Velocity - Time (v-t) Diagram of Exp. 2

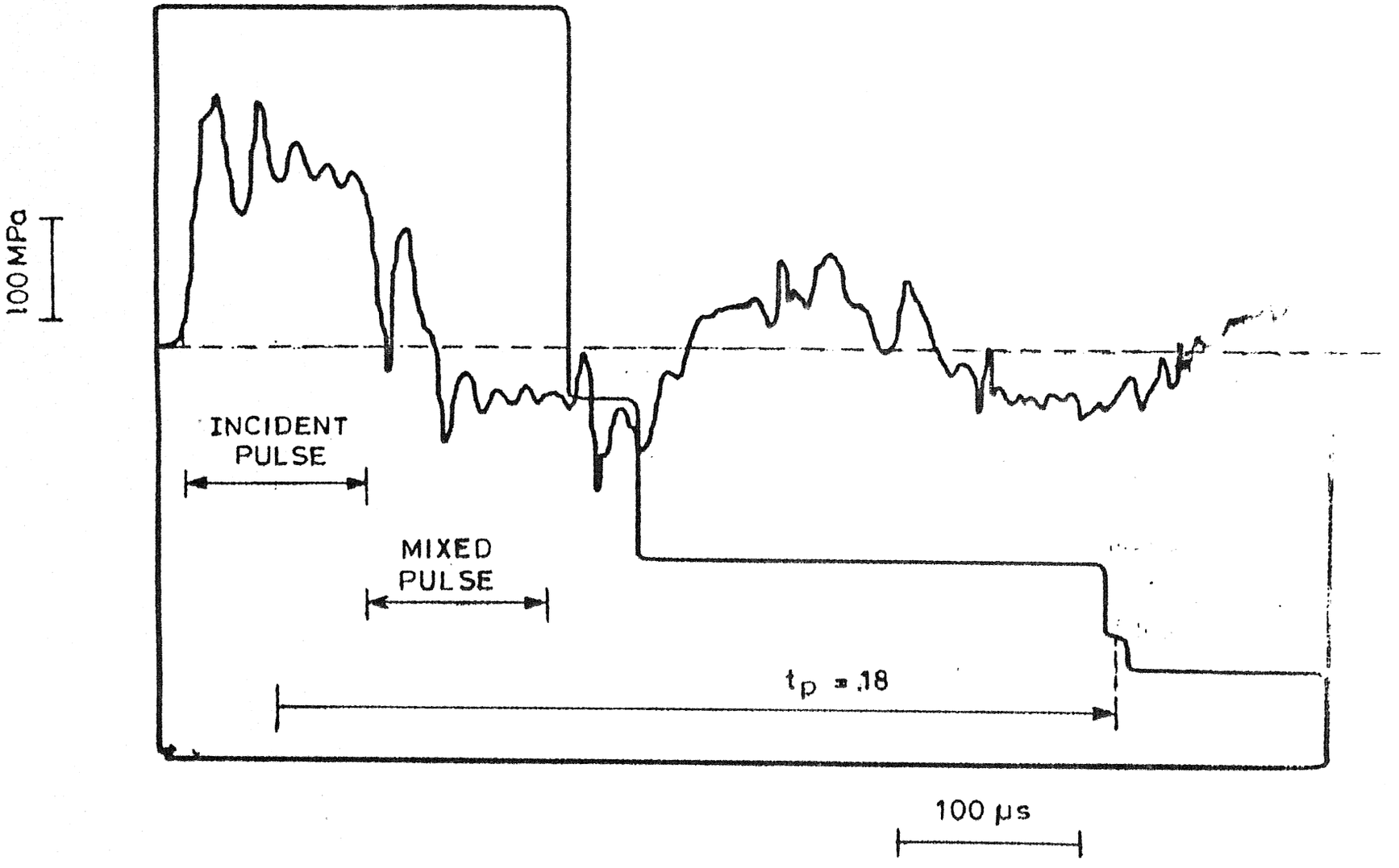

Fig. 5.13. Transient Stress and Crack Propagation Record of Exp. 3 at Straingauge S_i

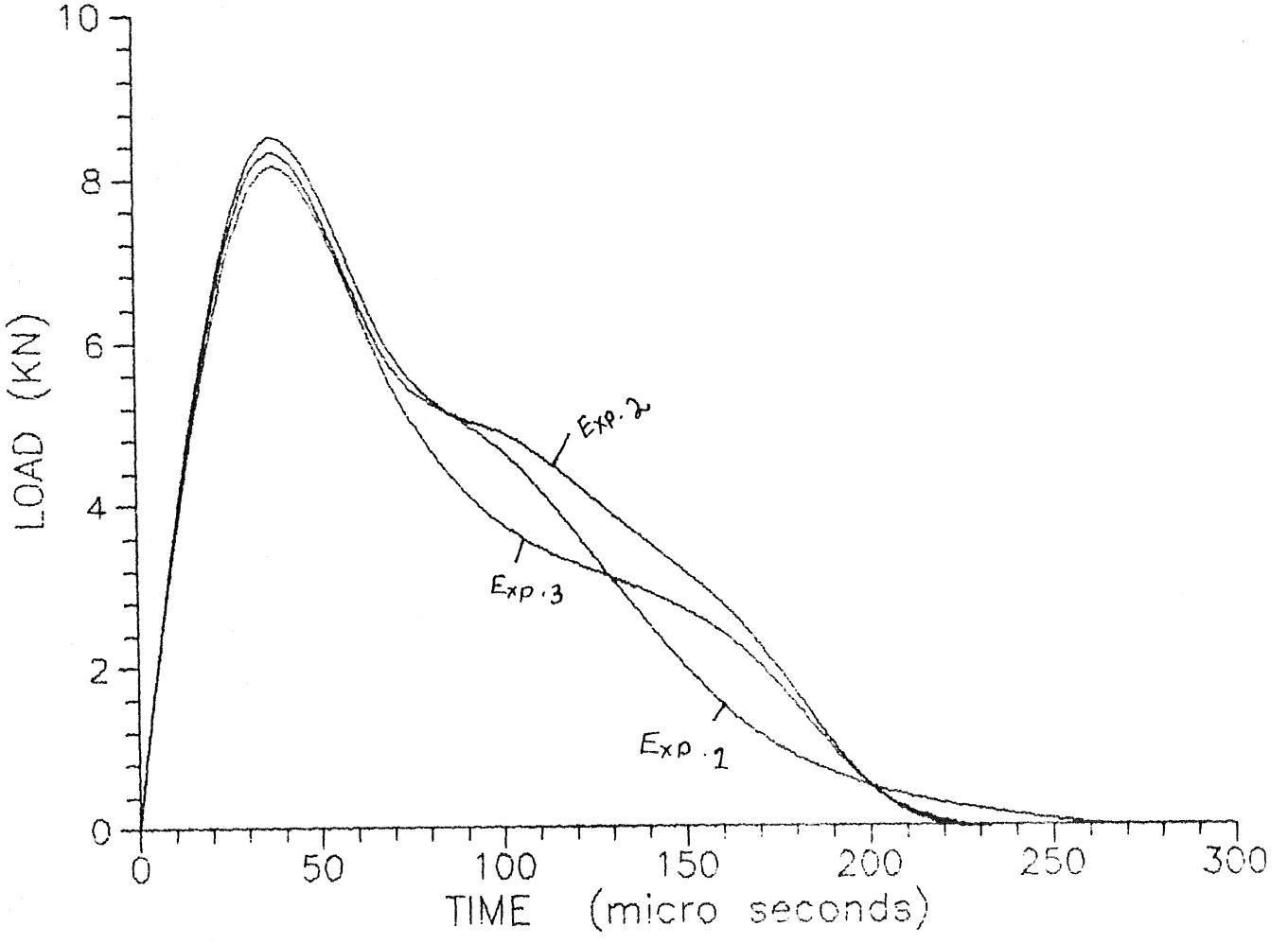

Fig. 5.14 Load - time (p-t) relationship of all experiments

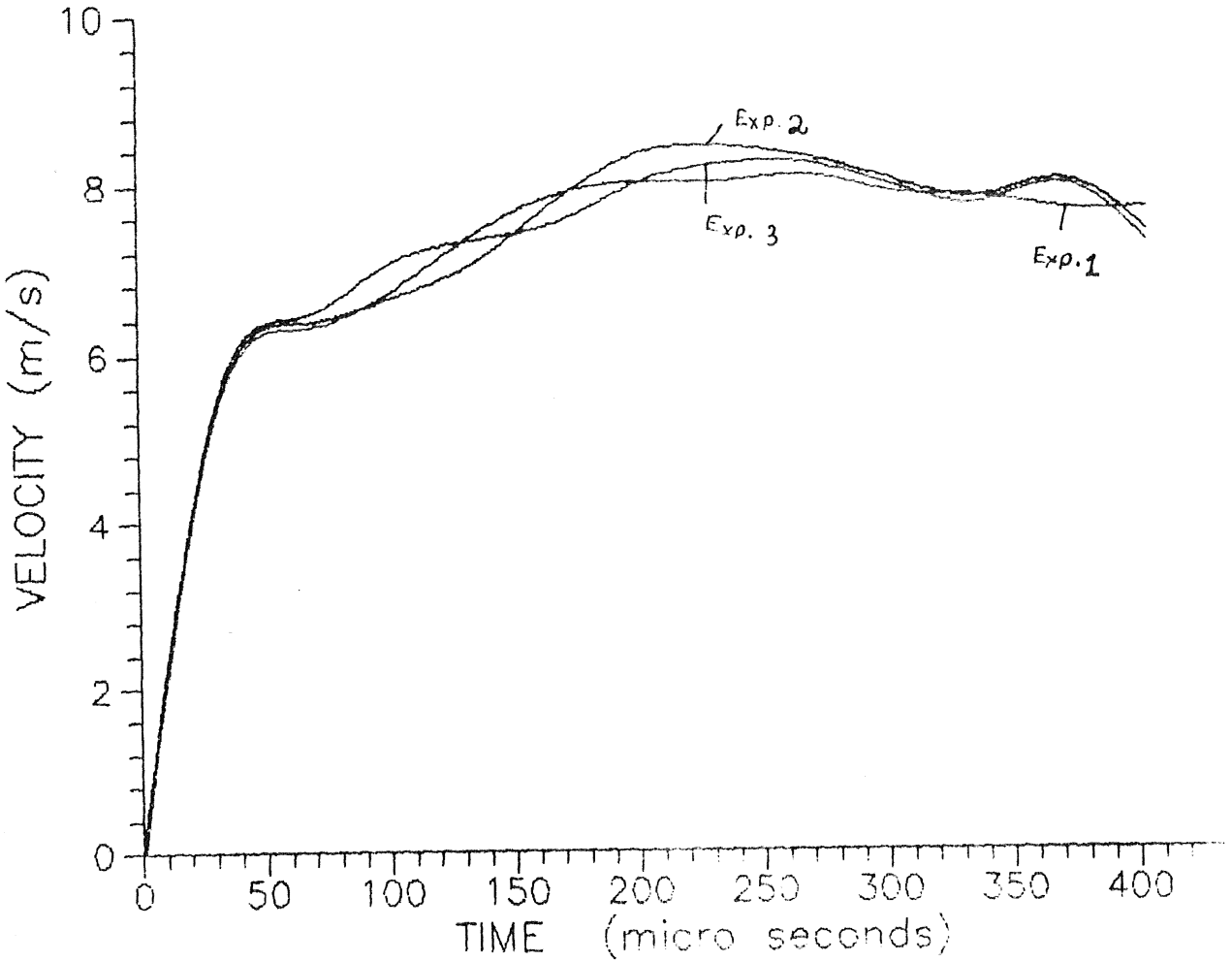

Fig. 5.15 Velocity - Time (v-t) relationship of all experiments

Table 5.1 Results of the Experiments

Expt.No.	$\dot{a}$ (m/s)	t_p (μs)	CCTE (J/m)
1	92	169Ø	17Ø.2
2	25	647	166.7
3	38	18ØØ	167.4

Initial crack length = 6Ø.ØØ mm.

CHAPTER 6

CONCLUDING REMARKS

Double cantilever beam specimen of glass fabric were loaded in Mode I. A starter crack was generated in the specimen by inserting mylar sheet during the casting. The crack was sharpened by extending it with a wedge under controlled conditions. Propagation gauge were bonded in front of crack tip to monitor the crack velocities. To each cantilever a long steel circular bar was attached. The lower cantilever was loaded dynamically by dropping a weight. The load and velocity of the cantilever tips were determined by recording stresses pulses through strain gauges bonded to the load bars.

The achieved crack velocities were in the range of 25 to 100 m/s. At these high runaway crack speed very small value of G_{Ic} was required to keep the crack moving. The G_{Ic} was so small that it was not measured by the techniques. It was estimated to be in the range of surface energies of solids that is 1 J/m^2 which is much smaller than 700 J/m^2 at quasistatic loading. However, it required a large energy per unit length of crack tip (CCTE) to accelerate the crack to the runaway velocities. The average value of CCTE was 168 J/m.

REFERENCES

1. Agarwal, B.D., and L.J. Broutman, "Analysis and Performance of Fibre Composites", John Wiley and Sons, New York, (1980).

2. Paul.E. Keary and Lary. B. Icewicz, Casey Shear and Jess Trostle, "Mode I Interlaminar Fracture Toughness of Composites Using Slender Double Cantilever Beam Specimen", J. of Composite Material, 19 (Mar. 1985), 154-177.

3. Wilkins, D.J., J.R. Eisenmann, R.A. Camin, W.S. Margolis and R.A. Benson, "Characterising Delamination Growth in Graphite Epoxy", Damage in Composite Materials, ASTM STP 775, 1982, 168-183.

4. Han, K.S. and J. Koutsky, "The Interlaminar Fracture Energy of Glass Fiber Reinforced Polyster Composites", J. Composite Materials, 15 (1981), 371-388.

5. Devitt, D.F., R.A. Schapery and W.L. Bradly, "A Method For determining the Mode I Delamination Fracture Toughness of Elastic and Viscoelastic Composite Materials", J. Composite Materials, 14, (1980), 270-285.

6. Guedra, D., D. Lang, J. Rouchon, C. Marais and P. Sigety, "Fracture Toughness in Mode I : A Comparison Exercise of Various Test Methods", VI ICCM, 3 (1987), 347-357.

7. De Charentenay, F.X. and M. Benzeggagh, "Fracture Mechanics of Mode I Delamination in Composite Materials", IV ICCM (1980), 186-197.

8. Narayan, M.D., "Energy Release Rates in Delamination Crack Propagation of Glass Fabric Reinforced Composites", M. Tech. Thesis, 1988, IIT Kanpur.

9. Savanur, R.A., "Experimental Evaluation of Dynamic G_I For The Interlaminar Crack Propagation in Fibre Composites", M.Tech. Thesis, 1989, IIT Kanpur.

10. Theodore, N. And Bless, S.J., "High Strain Rate Tension Testing", Metal Hand Book 9th edition, Vol. 8, Mechanical Testing ASM, June 1985.

11. Niordson, F.I., "A Unit For Testing Materials at High Strain Rates", Exp. Mech. Vol. 5, 1965, p. 29-32.

12. Hoggatt, C.R. and Recht, R.F., "Stress-Strain Data Obtained at High Strain Rates Using an Expanding Ring", Exp. Mech., Vol. 9, 1969, p. 441-448.

13. James ,W.D. and William ,F.R. ," Experimental Stress Analysis " McGraw Hill Kogakusha ,International Student Edition , Edition 2 (1978).

14. Takeda, N., Sierakowski, R.L., Ross, C.A. and Malvern, L.E., "Delamination-crack Propagation in Ballistically Impacted Glass/Epoxy Composite Laminates", Experimental Mechanics 22, (1982), p. 20-25.